Characterization of immune cell infiltration in clear cell renal cell carcinoma

Doctoral thesis

to obtain a doctorate

from the Faculty of Medicine

of the University of Bonn

Almotasem Salah-M Hamad

from Albaida/Libya

2024

Written with authorization of

the Faculty of Medicine of the University of Bonn

First reviewer: Prof. Dr. med. Marita Toma

Second reviewer: Prof. Dr. Annkristin Heine

Day of oral examination: 14.08.2023

From the Institute of Pathology

Director: Prof. Dr. med. Glen Kristiansen

Table of Contents

List of abbreviations

ADCC	antibody-dependent cellular cytotoxicity
APCs	antigen-presenting cells
Bregs	regulatory B cells
CCL2	C-C motif chemokine ligand 2
CCL22	C-C motif chemokine ligand 22
CCR2	CC-chemokine receptor 2
ccRCC	clear cell renal cell carcinoma
CTLA-4	cytotoxic T-lymphocyte-associated Protein 4
CTLs	cytotoxic T lymphocytes
ESKD	end-stage kidney disease
HLRCC	hereditary leiomyomatosis and renal cell carcinoma
HPF	high power field
ICIs	immune check point inhibitors
IFN-γ	Interferon gamma
IRAEs	immune related adverse effects
ISUP	international society of urological pathology
KIR	killer cell immunoglobulin-like receptor
NCAM	neural cell adhesion molecule
NK cells	natural killer cells
NKT cells	natural killer T cells
PD-1	programmed cell death protein 1
PD L1	programmed cell death-ligand 1
RCC	renal cell carcinoma
SRs	scavenger receptors

TAM	tumor associated macrophages
TCR	T-cell receptor
TIAI	tumor infiltration ability index
TIICs	tumor infiltrating immune cells
TKIs	tyrosine kinase inhibitors
TNF-α	tumor necrosis factor alpha
Tregs	regulatory T cells
VEGF	vascular endothelial growth factor
VHL	Von Hippel Lindau

1. Introduction

1.1 Epidemiology and risk factors

With about 400 000 cases yearly worldwide, accounts the renal cell carcinoma (RCC) for about 3 % of all adult cancers. Epidemiological studies show an increasing rate (Dutcher, 2019; King et al., 2014; Rassy et al., 2020). RCC accounts for around 90 % of the cases of renal kidney cancers (Rasmussen, 2013). Obesity, older age, diabetes, hypertension and cigarette smoking are risk factors the development of RCC, whereby these risk factors are also considered as risk factors for chronic kidney disease. From another side patients with end-stage kidney disease (ESKD) have a prevalence of 4.2 % for developing RCC (Henriksen and Chang, 2020). Among the chemical substances known to be associated with carcinogenesis ,trichlorethlyen was found to be associated with RCC more than to other cancer types (Gray and Harris, 2019).

About 3 % to 5 % of RCC occurs based on hereditary RCC syndromes, with Von Hippel Lindau (VHL) disease as the most common hereditary RCC syndrome (Dutcher, 2019 ; Gray and Harris, 2019). Mutations in the VHL gene could be found in more than 90 % of RCC cases. VHL gene mutations or loss can lead to the accumulation of the intracellular proteins HIF-1 alpha and HIF-2 alpha. These proteins can serve as transcription factors leading to activations of genes that induce the angiogenesis (Rassy et al., 2020).

1.2 Prognosis

Early stages of RCC are usually asymptomatic, which resulted in delayed diagnosis in the past. The typical clinical manifestations were flank pain, abdominal mass and hematuria. Nowadays, most cases of RCC are discovered by coincidence through medical imaging. (Dutcher, 2019; Gray and Harris, 2019).

The five-year survival for kidney cancer is about 76 %. Patients with a stage I of the disease have a five-year survival of nearly 93 %. Patients in stage II/III of the disease have a five-year

survival of 72.5 %. The prognosis worsens in stage IV with about 12 % patients surviving 5 years after diagnosis (Padala et al., 2020).

About 15-30 % of the RCC patients have an advanced stage at the time of the diagnosis and 20-30 % develop distant metastases in the follow-up (Dabestani et al., 2016; Rasmussen, 2013; Rassy et al., 2020; Siegel et al., 2018).

The most common sites of metastasis in RCC are the lungs followed by the bones, liver and brain (Dutcher, 2019).

Prognostic factors in RCC can be subclassified into anatomical, clinical, histological and molecular factors (EAU Guidelines, EAU-RCC-Guidelines-2022 (uroweb.org)). Anatomical factors comprise the localization, tumor size, lymph node metastases, vessel invasion, fat capsule invasion, adrenal invasion or invasion of other organs as well as distant metastases. These factors are all included in the TNM classification (Wittekind, 2020). Beside the TNM stage, the prognosis could be affected by histological factors like tumor subtype (clear cell, papillary or chromophobe differentiation), tumor grading and the presence of necrosis. Additionally, the presence of sarcomatoid or rhabdoid morphology has also been shown to be associated with poor prognosis (Warren and Harrison, 2018). Among the clinical prognostic factors, a low haemoglobin level, higher serum level of lactate dehydrogenase, and higher corrected calcium level in serum are all parameters associated with poor prognosis (Gray and Harris, 2019).

A previous study by the Memorial Sloan Kettering Cancer Centre identified the low Karnofsky performance status, a high level of LDH, a low serum hemoglobin and serum calcium as well as the absence of the nephrectomy as risk factors for and according to these factors they defined three prognostic groups of patients (Motzer et al., 1999).

In recent years, more studies have shown how the immune cell infiltration of the RCC tissue can affect the prognosis. Aside from the lower TNM stage, a favourable immune score was found to be associated with prolonged better disease-free survival, progression-free survival,

and overall survival (Selvi et al., 2020). Also the higher expression of programmed cell death-ligand 1 (PD-L1) in RCCs is associated with poor prognosis (Parikh and Bajwa, 2020).

1.3 Diagnosis and screening

In case of RCC suspicion, the examination by contrast enhanced CT or abdominal ultrasound plays an important role in the initial diagnosis of the disease. Abdominal CT can also provide information about the status of the contralateral kidney, the venous involvement and the enlargement of the regional lymph nodes. The diagnosis is confirmed through a histological examination after nephrectomy or partial resection. Magnetic resonance imaging is recommended in case of CT contrast medium allergy or in pregnancy. If lung metastases are suspected, chest imaging is indicated. Signs of bone or brain metastasis require further investigation through bone scan, brain CT, or MRI. With the exception of patients with hereditary renal cancer syndromes, there are generally no screening examinations for RCC (Gray and Harris, 2019; (EAU Guidelines, EAU-RCC-Guidelines-2022 (uroweb.org)).

1.4 Treatment

The surgical resection of the tumor is the first therapy option in the early stage of RCC. The surgery is undertaken through partial or total nephrectomy. The decision to conduct a radical or partial nephrectomy depends on some factors, whereby a tumor size larger than 3cm, a non-pre-existing renal insufficiency and a good function of the contralateral kidney are all factors that overweight the decision to carry out total nephrectomy (Gray and Harris, 2019). The oncological outcome in terms of overall survival after partial naphrectomy in T1 tumors equals that from radical nephrectomy and should therefore be preferred in this tumor stage (EAU Guidelines, EAU-RCC-Guidelines-2022 (uroweb.org)). Other therapy options in case of small renal masses could be thermal therapy cryotherapy or radiofrequency ablation (Gray and Harris, 2019). RCC is highly resistant to traditional chemotherapeutics (Buti et al., 2013). Tyrosine kinase inhibitors (TKIs) that inhibit the angiogenesis are used to treat advanced RCC and have improved the prognosis in this patient group (Rassy et al., 2020). Recent years have shown the arrival of new therapy strategies, combining immune checkpoint inhibitors (ICIs), which act through inhibition of programmed cell death protein 1 (PD-1) PD-

L1 or cytotoxic T-lymphocyte-associated protein 4 (CTLA-4), leading to induction of the T cells against the cancer cells (Wolf et al., 2020).

RCC is considered as highly immunogenic tumor, which could clarify its higher response to therapy with ICIs. The application of ICIs in recent years has shown a major success in improving the outcome in patients with advanced RCC. One or a combination of two ICIs as well as the combination of ICI and TKI are now in the first-line therapy of advanced and metastasized renal cancer (Choueiri et al., 2021; Parikh and Bajwa, 2020).

Nivolumab – a PD-1 blocker – is used as first-line therapy to treat the intermediate and high-risk group of metastatic RCCs (MSKCC criteria) and revealed the best response rate. Ipilimumab – a CTLA-4 inhibitor – has been shown to improve the outcome when added to nivolumab and it has become the first-line therapy in this patient group (Parikh and Bajwa, 2020).

Another clinical study in phase III (IMmotion151) achieved positive results with the combination of atezolizumab (PD-L1 inhibitor) and bevacizumab (VEGF-antibody) (Rini et al., 2019).

On the other side, the application of ICIs can lead to immune-related adverse effects (IRAEs). IRAEs usually appear in the first weeks of the treatment.

Fatigue, pruritus and rash are common IRAEs, that can be well tolerated in most cases. Limitation factors of the ICI treatment include some severe IRAEs like, hypophysitis, myasthenia gravis, myocarditis, pneumonitis, autoimmune hepatitis, adrenal insufficiency, type 1 diabetes mellitus colitis or nephritis. However, these IRAEs are not common (Parikh and Bajwa, 2020).

Nevertheless, the application of the ICIs in the therapy of RCC has increased the importance of understanding the tumor-infiltrating immune cells in RCC.

1.5 Pathology

There are many histological types of the RCC. The WHO classification of the RCCs is based on morphological and molecular features. Clear cell renal cell carcinoma (ccRCC) is the most common subtype, accounting for about 70-90 % of cases. ccRCC usually express cytokeratin

and vimentin. However this histologically most frequent type is generally negative for cytokeratin 7 (Warren and Harrison, 2018).

The second most frequent type with about 10-15 % of RCC cases is the papillary RCC, which can be divided by the recent WHO classification into type I (less aggressive) and type II according to genetic alteration. Other types are the chromophobe (makes about 3-5 % of RCC and usually has a good prognosis) the medullary RCC the collecting duct carcinoma RCC (a rare form of RCC accounting for about 1-2 % of cases) and the translocation RCC (Dutcher, 2019; Warren and Harrison, 2018).

Furthermore, the 2016 WHO classification added five new subtypes of the RCC, proposed by the International Society of Urological Pathology (ISUP) on Vancouver consensus meeting in 2012: hereditary leiomyomatosis and RCC syndrome-associated RCC (HLRCC), the SDH deficient RCC, tubulocystic RCC, acquired cystic disease-associated RCC and clear cell papillary RCC. About 5 % of RCCs remains unclassified due to difficult categorization (Dutcher, 2019; Warren and Harrison, 2018).

1.6 TNM

Like most cancers, the TNM classification also plays a central role in choosing the therapy plan and evaluating the prognosis in RCC. Besides the tumor size, the T-stage involves the infiltration of the perirenal fat tissue, the Gerota's fascia, the ipsilateral adrenal gland, the renal vein or the vena cava. The recent edition of this classification system is the 8th edition (Wittekind, 2020).

Tab. 1: TNM classification of the RCC.

T stage	T1 smaller than 7 cm • T1a < 4 cm • T1b > 4 cm < 7 cm T2 larger than 7 cm • T2a >7 cm < 10 cm • T2b > 10 cm T3 • T3a infiltration of the perirenal fat tissue or macroscopically infiltration of a renal vene • T3b infiltration of the inferior vena cave below the diaphragm • T3c infiltration of the inferior vena cave above the diaphragm T4 • Infiltration of Gerota's fascia or the ipsilateral adrenal gland • Infiltration of other organs
N stage	N0: no lymph node involvement N1: involvement of at least one lymph node
M stage	M0: no distant metastases M1: distant metastases

1.7 Grading

In the past, the Fuhrman grade system was the standard for grading of RCCs (Fuhrman et al., 1982). Grade 1 tumors have small nuclei (about 10µm) with not clearly visible or absent nucleoli. In grade 2, the nuclei are larger (about 15µm) and the nucleoli are visible at large magnification (400 X). The nucleoli are even larger in grade 3 (about 20µm) with a noticeable irregular outline and larger nucleoli (already visible at 100 X magnification). In grade 4, tumors exhibit similar characteristics of grade 3 with the addition of unusual pleomorphic nuclei and heavy chromatin clusters.

In recent years the WHO/ISUP grading system has acquired an increasing application for

ccRCC and papillary RCC. The new WHO/ISUP grading system should have a higher reproducibility than the classical Fuhrman grade system. The WHO/ISUP grading system also has four grades. The grades from 1 to 3 are given according to the prominence of the nucleoli. In grade 1, the nucleoli are not identifiable at 400 X magnification. In grade 2, small nucleoli can be distinctly detected at 400 X magnification. In grade 3, the nucleoli are already visible at the 100 X magnification. The revealing of pleomorphic and atypical cells with rhabdoid or sarcomatoid differentiation or showing extreme nuclear pleomorphism with clumping of chromatin defines grade 4 (Delahunt et al., 2013; Warren and Harrison, 2018).

1.8 Tumor-infiltrating immune cells

Studying the immune system response to cancer has always been a massively investigated field. As the ccRCC is considered a highly immunologic tumor, investigating the immune response and the nature of the tumor infiltrating immune cells (TIICs) in ccRCC holds strong importance. The tumor microenvironment contains different amount of special immune cell subtypes. In the present study we will investigate the tumor infiltration through the T lymphocytes, the B lymphocytes, the natural killer cells and the macrophages by immunohistochemistry with the following surface markers: CD3, CD4, CD8, CD20, CD56, CD68 and CD103.

1.8.1 CD3+ lymphocytes

CD3 is expressed in almost all T-lymphocytes and it is applied in studies as general marker for T-lymphocytes (Arnett et al., 2004). Several studies could show that a rich CD3 tumor infiltration is associated with favorable prognosis in RCC (Guo et al., 2019; Selvi et al., 2020; Stenzel et al., 2019).

Investigations into the relationship between CD3 cell tumor infiltration and the effectiveness of the immunotherapy have showed that a higher CD3 density in the centre of the tumor could predict therapy response to nivolumab. Responders to nivolumab therapy also had a significantly higher PD-1 positive immune cells in the tumor center (Stenzel et al., 2019).

1.8.2 CD4+ lymphocytes

CD4 helper cells plays an important role in the activation of B-lymphocytes to antibody-producing lymphocytes (Nutt et al., 2015). CD4+ cells can also increase the bactericidal function of the macrophages (Kovaleva et al., 2016).

On the other side $CD4^{+}Foxp3^{+}$ regulatory T cells (Tregs) are a subtype of the CD4+ cells with an immunosuppressive effect. They play an important role against excessive immune reaction. They secrete immunosuppressive cytokines leading to inhibition of the antigen-presenting cells (APCs) (Sasidharan Nair and Elkord, 2018).

In ccRCC, higher tumor infiltration through resting memory CD4 cells has shown to be associated with better prognosis, while a higher density of Tregs has been associated with a poor outcome (Zhang et al., 2019).

Daurkin et al., (2011) showed that the tumor-associated macrophages in RCC could induce the expression of FOXP3 and CTLA4 in the T-cells causing an immunosuppressive response.

1.8.3 CD8+ lymphocytes

CD8 is a surface marker for cytotoxic T-lymphocytes (CTLs). CTLs play an important role in defence against infections as well as various malignancies (Raskov et al., 2021).

There are contradictory results in the literature regarding the association between the CD8+ T-cell infiltration and the prognosis in RCC, whereby a higher CD8+ T-cell infiltration in the RCC could be shown to be associated with poor diagnosis (Stenzel et al., 2019; Guo et al., 2019). On contrast, the study by Selvi et al. (2020) could show an association between higher CD8+ T-cell infiltration density and favourable prognosis. In chromophobe renal cancer, the abundant CD8+ T-cell infiltration was associated with better overall survival (Zhang et al., 2019).

A higher CD8+ T-cell density in the invasive margin of the tumor has shown to be associated with response to therapy with nivolumab (Stenzel et al., 2019).

1.8.4 CD20+ cells

CD20 is used as marker for B-lymphocytes. It is already expressed in the pre B-cell stage and becomes lost during plasma cell differentiation (Cragg et al., 2005). B-lymphocytes initiate in the bone marrow from the lymphoid progenitors and move into the secondary lymph organs forming germinal centers, where they can proliferate and produce a immunoglobulin class switch to IgG, IgA or IgE during differentiation into plasma cells (Shen et al., 2016).

Mature B- cells can be divided into follicular B cells, marginal B cells and B1 cells. Follicular B cells comprise the majority of the B-cells and they can be found in the lymphoid follicles of the lymph nodes and the spleen. Marginal B cells are located near the marginal sinus of the spleen. B1 cells are located in the pleural and the peritoneal cavity (Nutt et al., 2015).

The antibodies produced by the plasma cells can play an important role in opposing the tumor antigens, but the role of the B-cells against the cancer cells is not well understood (Shen et al., 2016).

It has been shown that rich B-lymphocytes infiltration is associated with better prognosis in several types of cancers (Ladányi, 2015; Sharonov et al., 2020). In the study by Kobayashi et al. (2014), it could be shown that the transfer of B-cells in B-cell linker protein deficient mice leads to improving the prognosis of the melanoma.

On the other side, several studies could show that some subtypes of B-cells – especially the regulatory B-cells (Bregs) – can have a negative impact in tumor infiltration through immune suppression (Wei et al., 2016; Zhou et al., 2016).

B10 cells are a subpopulation of B-lymphocytes that can produce IL-10, an inhibitory interleukin leading to suppression of the T-cell differentiation resulting in inhibition of the cancer immune response. The number of IL-10 producing cells in ovarian cancer was found to be correlated with the clinical stage (Wei et al., 2016).

Further studies could reveal that the immunosuppressive component of the B-cells can occur through interaction with T-cells. It has been shown that Bregs can convert the CD4+CD25- cells into Tregs in tongue squamous cell carcinoma (Zhou et al., 2016). In another study, the

number of the IL10+ B-cells was positively correlated the frequency of the $Foxp3^+$ $CD4^+$ T-cells in the ascites of patients with ovarian cancer and the coculture of T cells with tumor B cells led to reducing its amount of secreted Interferon gamma (IFN-γ) (Wei et al., 2016).

In the RCC, the B lymphocytes seems to have a positive impact on the prognosis. In the study by Stenzel et al. (2019), the B-cell infiltration in the ccRCC was associated with with favourable cancer specific survival.

1.8.5 CD56+ cells

CD56 positive cells – also called natural killer (NK) cells – are cytotoxic lymphocytes that play an important role in eliminating viral infected cells or tumor cells. They eliminate these cells without prior exposure. Once activated, they can release perforin and granzyme granula, leading to lysis of the targeted cells. NK cells can also recognize antibody-covered cells through its Fc-receptor CD16, a process known as antibody-dependent cellular cytotoxicity (ADCC). On the other hand, the NK cells express inhibitory receptors preventing attacking the healthy human cells through recognizing of MHC class I and other surface molecules. The most important inhibitory receptor family is the killer cell immunoglobulin-like receptor (KIR) family (Wagner et al., 2019).

Studies on the CD56 infiltration have revealed an association between a higher infiltration and a favorable prognosis in several tumors (Fregni et al., 2012; Senovilla et al., 2012). It could also be shown, that the NK cell infiltration correlates with the response to anti-PD1 immunotherapy (Cózar et al., 2020), although in several tumors the NK cells – especially the intratumoral NKs – have been shown to produce a lower amount of IFN-γ and tumor necrosis factor alpha (TNF-α). In breast cancer the NK cells have been shown to express lower CD16 density on their surface (Cózar et al., 2020; Fregni et al., 2012; Petricevic et al., 2013).

Natural killer T (NKT) cells are a subtype of the NK cells, which also express the T-cell receptor (TCR) and CD4 or CD8 receptors (Senovilla et al., 2012).

1.8.6 CD68+ Macrophages

CD68 is glycoprotein, which is expressed in the cells of the monocyte/macrophage linage. Macrophages belong to the mononuclear-phagocytose lineage, together with the myeloid dendritic cells, osteoclasts and microglia (Chistiakov et al., 2017). CD68 has also been shown to be low expressed on some cells outside the mononuclear- phagocyte lineage, like fibroblasts and endothelial cells (Gottfried et al., 2008). Macrophages are known to have a clearance function, since they are able to phagocyte cell detritus. They have several scavenger receptors (SRs), through which they can recognize different ligands (Chistiakov et al., 2017).

The macrophages can be divided into M1 and M2 macrophages. The M1 macrophages have been shown to have a proinflammatory effect. M2 machrophages have an anti-inflammatory effect leading to promote the tumor growth. They can secrete anti-inflammatory cytokines like IL-10, leading to immunosuppressive effects (Komohara et al., 2011). Tumor associated macrophages (TAMs) are also able to produce vascular endothelial growth factor (VEGF) promoting the angiogenesis in tumor tissue (Toge et al., 2009). It could also be shown that the interaction between the macrophages and the tumor cells, can lead to differentiation of the macrophages into the M2-typ, leading to tumor growth induction. TAMs have been shown to induce tumorogenesis in many tumors (Komohara et al., 2011).

In the study by Stenzel et al. (2019) higher macrophage infiltration of the tissue of ccRCC was associated with poor prognosis compared with patients with low macrophages infiltration. Specific investigation into the M2 macrophages in RCC showed an association between high infiltration of M2 macrophages and poor overall survival (Komohara et al., 2011).

Different results were found in the colorectal cancers. Here a higher M2 macrophage density was associated with better prognosis (Nagorsen et al., 2007).

Another study on pan-TAMs showed a correlation with better prognosis in colorectal cancer, whereby a low TAM infiltration was associated with lymph node metastasis, and a higher TAM infiltration was correlated with no distant metastasis status (Zhao et al., 2019).

Macrophages accumulate in the cancerous tissue attracted by chemotactic factors. It has been shown that a RCC can produce a higher amount of C-C motif chemokine ligand 2

(CCL2), which is believed to recruit monocytes from the peripheral blood. These monocytes express it sides the CC-chemokine receptor 2 (CCR2) (Daurkin et al., 2011).

Interestingly some cancer cells – especially metastatic cancer cells – can express macrophage antigens like CD68. This overexpression of the macrophage antigens helps these cancer cells to escape macrophage-mediated phagocytosis (Chistiakov et al., 2017).

1.8.7 CD103+ cells

CD103 is a subunit of the integrin complete heterodimeric molecule αEβ7 and it is involved in cell adhesion migration and homing of lymphocytes (Wang et al., 2015). CD103 is expressed in the immune cells mostly in the CTLs but also in dendritic cells and NK cells (Djenidi et al., 2015; Xiao et al., 2019).

In a study of CD103+ cells in the bladder cancer, it has been shown that a higher density of the CD103+ cells is associated with a better outcome. It could also be demonstrated that the majority of the CD103+ cells were CD8 positive. The CD103 positivity of the CD8 cells was more frequent intratumorally than in the stromal region (Wang et al., 2015).

In fact, CD103+ tumor infiltration have been shown to be associated with better outcome in several cancer types (Broz et al., 2014; Djenidi et al. 2015; Xiao et al., 2019). Interestingly, Djenidi et al. (2015) could that the CD8 cells that were positive for CD103 revealed a higher granzyme B concentration than CD103- cells.

1.9 Purpose of the study

The aim of this study was to characterize the immune cell infiltration in ccRCC and distant metastases. We aimed to answer following questions.

1. How is the peritumoral immune cell infiltration (CD3, CD4, CD8, CD20, CD68 and CD103+ cells) in RCC according to clinico-pathological characteristics?
2. How is the intratumoral immune cell infiltration (CD3, CD4, CD8, CD20, CD68 and CD103+ cells) in RCC according to clinico-pathological characteristics?
3. Are there differences in the primary tumors and paired distant metastases?
4. Correlates the CD68+ cell infiltration with clinico-pathological characteristics?

5. Correlates the CD56+ cell infiltration with clinico-pathological characteristics?
6. How correlates the different immune cell subtypes with each other?

2. Material and Methods

Formalin-fixed, paraffin embedded material from 50 patient who underwent partial/radical nephrectomy for renal cancer between 2003-2014 in the Department of Urology, University Hospital Bonn were included in the study. All patients had the diagnosis of ccRCC. The study was approved by the ethic committees of the University Hospital Bonn (EK 233/20). We chose 28 ccRCC patients with distant metastases (M1) for the study. As a control group we selected 22 patients without any distant metastases (M0 stage). All of the metastases in the M1 patients were confirmed histopathologicaly, aside from two, which were diagnosed clinically after the nephrectomy. Patient data for this study and pathological tumor parameters are summarized in Table 2.

Tab. 2: Clinico-pathological characteristics of the patients included in the study.

	No. of patients
M-Status	
M1	28
M0	22
Distant metastases	22
Grading	
G1	1
G2	36
G3	10
G4	3
pT stage	
T1/T2	20
T3/T4	30
Age	
Range:	38-79
Median:	68
Sex	
Female:	22
Male:	28

2.1 Methods

2.1.1 Immunohistochemistry

The stainings were performed automatically in the autostainer 480S (Fa. Medac). The tumor tissues were fixed with 4% buffered formalin and embedded in paraffin. After choosing a representative tumor block, the block was sectioned at 2-3 µm and the sections were mounted on Super Frost Plus™ adhesion slides. The slides were dried at 65 degrees for one hour in a slide incubator. For the epitope retrieval – which can be caused through the formalin fixation– a heat pre-treatment was achieved in PT-module with PH of 6.0 at 99 degrees for 20 minutes. After washing the slides in wash buffer and distilled water, the endogenous peroxidase was blocked with hydrogen peroxide (H_2O_2) for 10 minutes. The slides were washed and then incubated with the primary antibody for 30 minutes.

After washing the slides several times, the detection system with enhancer was applied, first the polymer and then the 3,3′-diaminobenzidine (DAB) for 8 minutes. The slides were washed again and then counterstained with hematoxylin, dehydrated using alcohol in increasing concentrations, cleared with xylol and mounted in a non-aqueous medium.

The following monoclonal antibodies were used to detect the immune cells of interest: pan T-cells (CD3, clone 565, Fa. Leica , Nr. NCL-L-CD3-565, dilution 1:50), T-helper cells (CD4, clone SP35 , Fa. Roche , Nr. 790-4425, ready to use antibody), CTLs (CD8; clone C8/1448 , Fa. Agilent , Nr. M 7103; dilution 1:50), B-lymphocytes (CD20; clone L26 , Fa. Agilent , Nr. M 0755, dilution 1:2000), NK cells (CD56; clone RCD56, Fa. Zytomed, Nr. RBK 050, dilution 1:100), macrophages (CD68; clone PG-M1, Fa. Agilent, Nr. M 0876, dilution 1:100) and tissue resident memory T-cells (CD103; clone EPR4 , Fa. Abcam , Nr. ab 129202, dilution 1:100).

2.1.2 Microscopic evaluation

For each patient we chose the tumor slides with the highest peritumoral immune cell infiltration. We counted the TIICs peritumoral and intratumoral manually for all of the immune cells of interest: CD3, CD4, CD8, CD20, CD56, CD68, and CD103. We selected under the microscope the regions with the highest immune cell infiltratation and the positive cells were

counted in five fields at the 400 X magnification. The intratumoral counting of the immune infiltrating cells occurred in the middle of the tumor, again in five fields at the 400 magnification. Next, we determined the peritumoral as well as the intratumoral average of the immune cell infiltration building the mean value of the 5 fields peri/intratumoral for each patient.

We also counted the immune cell infiltration in the 22 distant metastases, counting the number of positive cells in 5 fields in the middle of the metastasis at the 400 X magnification. We also calculated the average immune cell count of these five fields.

2.2 Statistical Analysis

The mean value was calculated for every group. Comparison between the groups were made using the student's t-test and Mann–Whitney U test. Correlation analyses between variable groups were determined by Pearson's correlation coefficient. P values < 0.05 were considered significant and <0.01 as highly significant. Statistical analysis were performed using IBM SPSS 25.0.

3. Results

3.1 Characterization of the immune cell infiltrate in ccRCC

3.1.1 Infiltration of CD3-positive T lymphocytes in ccRCC

We found a large number of CD3 positive lymphocytes intratumoral (mean: 65.7 cells/high power field (HPF), range: 7.4-365.8 cells/HPF) and peritumoral (mean: 106 cells/HPF, range:11.2-333.4 cells/HPF) in all cases of ccRCC (Fig 1).

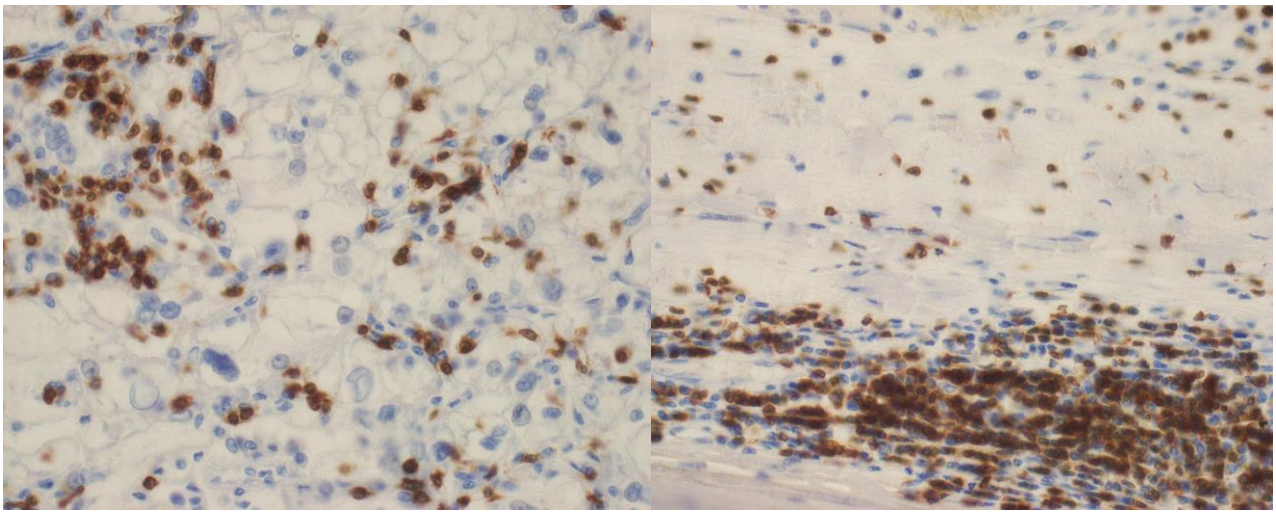

(A) (B)

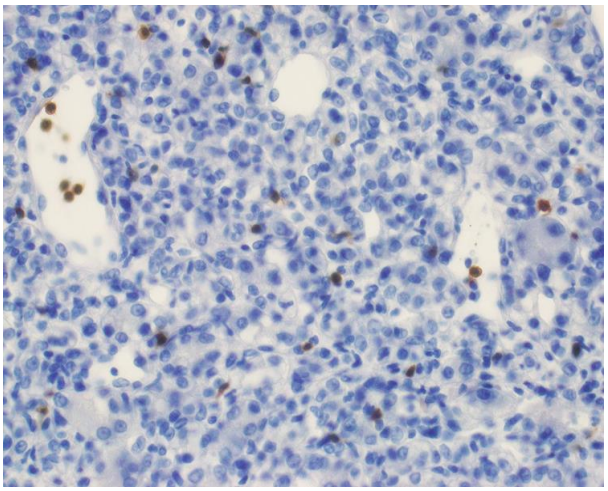

(C)

Fig. 1: Representative pictures of the immune cell infiltration in the primary ccRCC showing a high CD3-positive T-cell infiltration intratumoral (A) peritumoral (B) and in the distant metastasis (C) (x200 magnification).

3.1.2. Infiltration of CD4-positive T-helper cells in ccRCC

CD4 Infiltration revealed a rich infiltration in the majority of our cases (mean of the intratumoral infiltration: 30.8 cells/HPF, range: 1.4-226 cells/HPF, mean of the peritumoral infiltration: 55.7 cells/HPF, range: 10.8-161 cells/HPF) (Fig. 2).

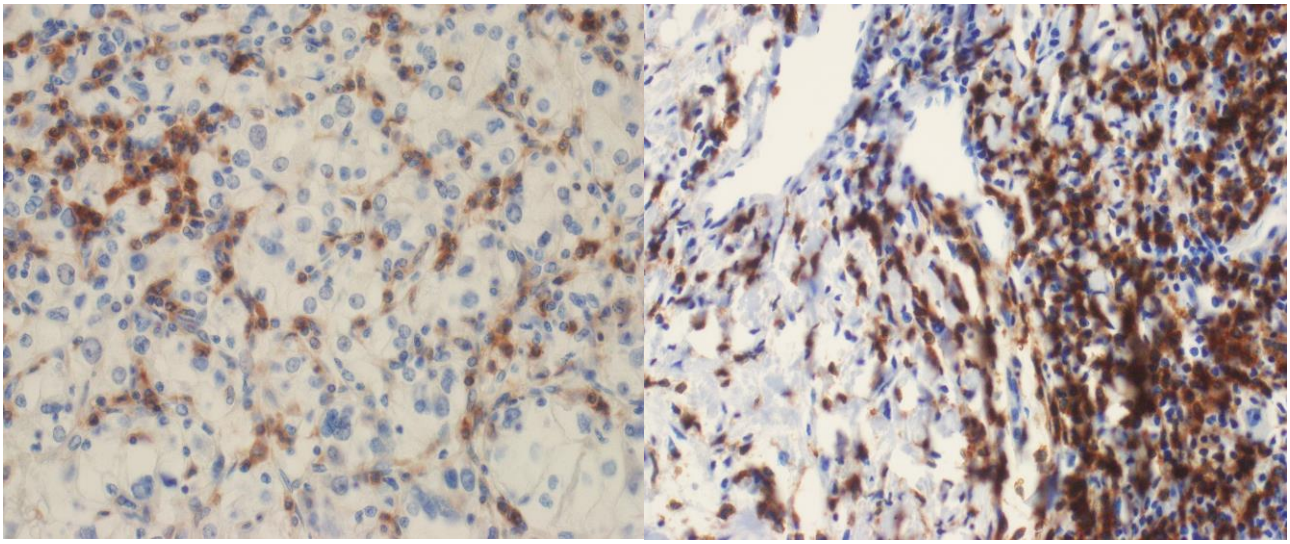

(A) (B)

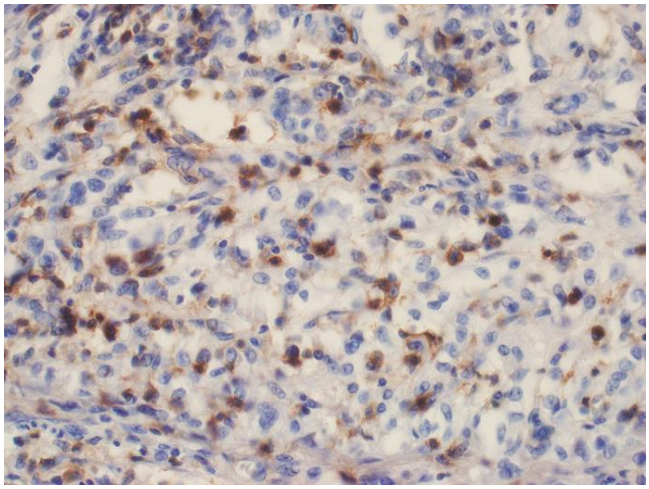

(C)

Fig. 2: Representative pictures of the immune cell infiltration in the primary ccRCC showing the CD4-positive T-cell infiltration intratumoral (A) peritumoral (B) and in the distant metastasis (C) (x200 magnification).

3.1.3. Infiltration of the CD8-positive T lymphocytes in ccRCC

CD8 T-cell infiltration was also abundant in most cases. The intratumoral CD8-positive T-cell infiltration showed a mean of 39.7 cells/HPF and range between 0.4 and 237 cells/HPF. The

peritumoral CD8-positive T-cell infiltration had a mean of 58.4 cells/HPF and a range between 0 and 128 cells/HPF (Fig 3).

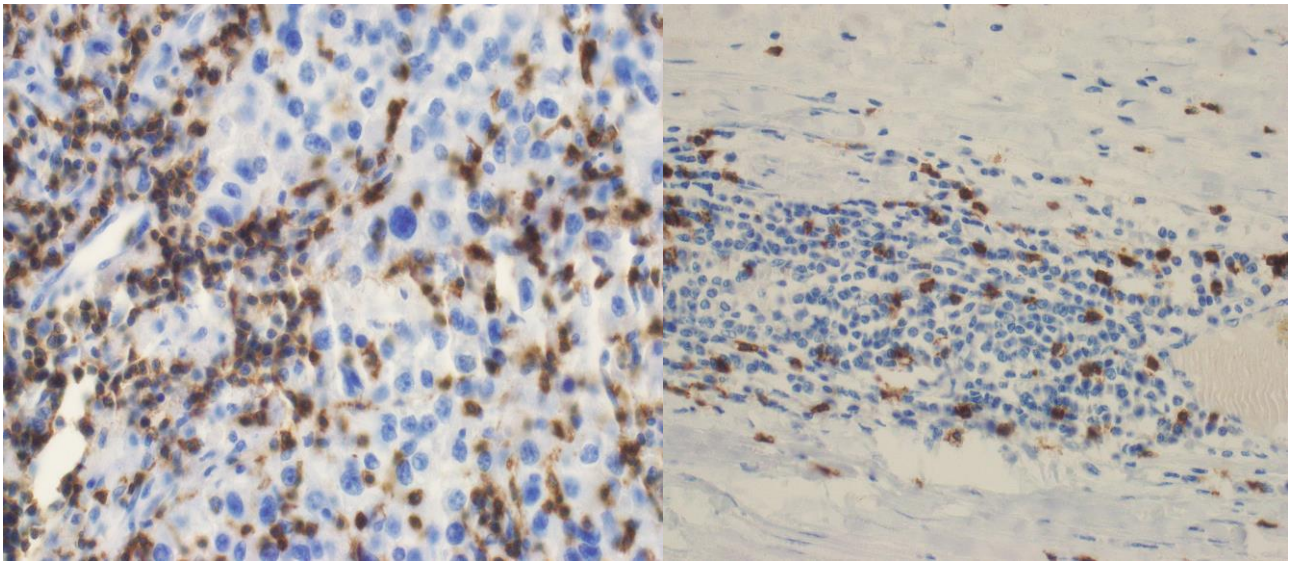

(A) (B)

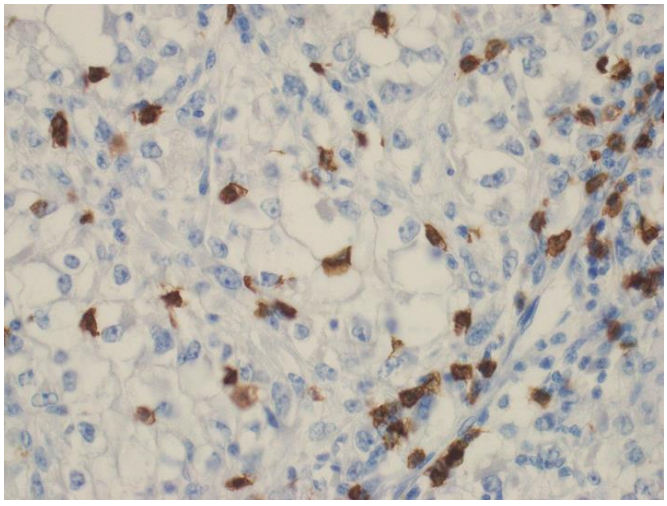

(C)

Fig. 3: Representative pictures of the immune cell infiltration in the primary ccRCC showing a high CD8-positive T-cell infiltration intratumoral (A) peritumoral (B) and in the distant metastasis (C) (x200 magnification).

3.1.4. Infiltration of the CD20-positive B-cell lymphocytes in ccRCC

Compared with the high number of intratumoral and peritumoral T-cell infiltration, the CD20-positive B-cell infiltration was very sparse. Especially the intratumoral CD20-positive B-cell infiltration showed a very low density (mean: 2.7 cells/HPF and range of 0-17 cells/HPF). The peritumoral CD20-positive B-cell infiltration showed a mean of 27.5 cells/HPF and range between 0.6 and 154 cells/HPF (Fig. 4).

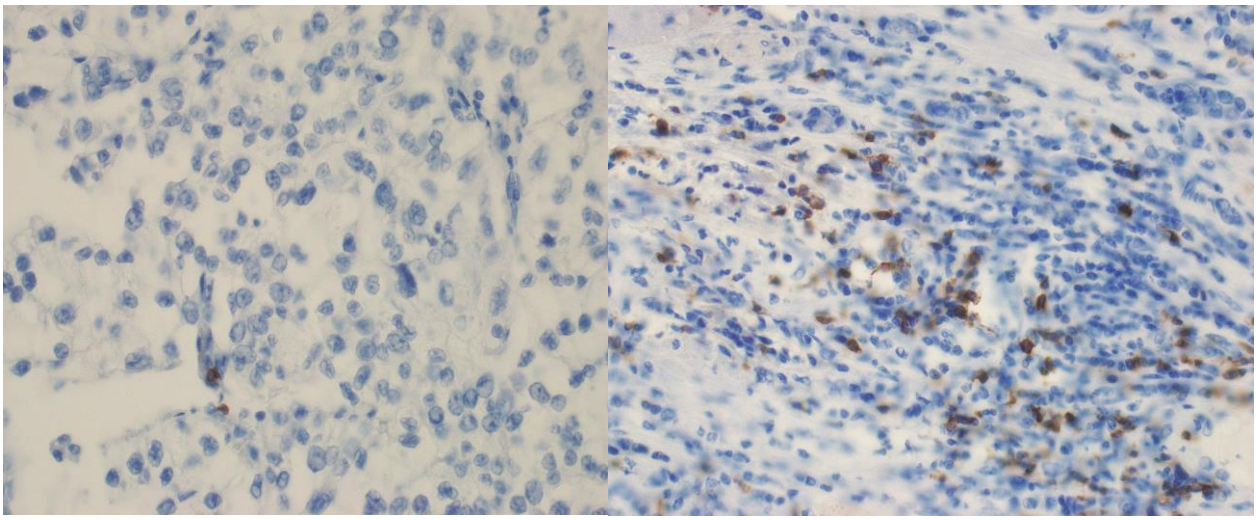

(A) (B)

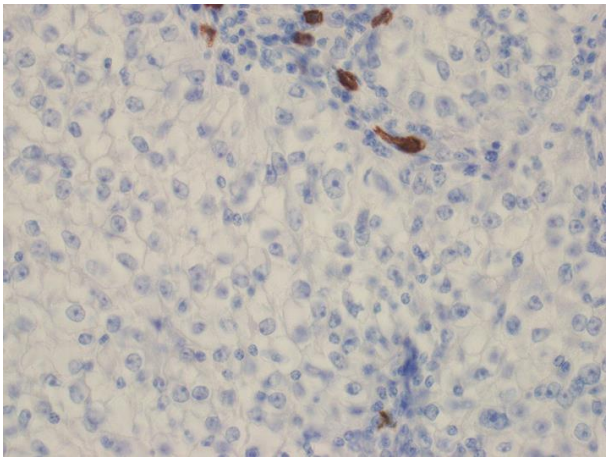

(C)

Fig. 4: Representative pictures of the immune cell infiltration in the primary ccRCC showing the CD20-positive B-cell infiltration intratumoral (A) peritumoral (B) and in the distant metastasis (C) (x 200 magnification).

3.1.5. Expression of CD56 in immune cells and tumor cells in ccRCC

We did not observe an abundant tumor infiltration of the CD56-positive cells (mean of the intratumoral CD56 cell infiltration: 4.2 cells/HPF, range: 0-28.2 cells/HPF; mean of the peritumoral infiltration 6.4 cells/HPF, range: 0-23.6 cells/HPF) (Fig 5).

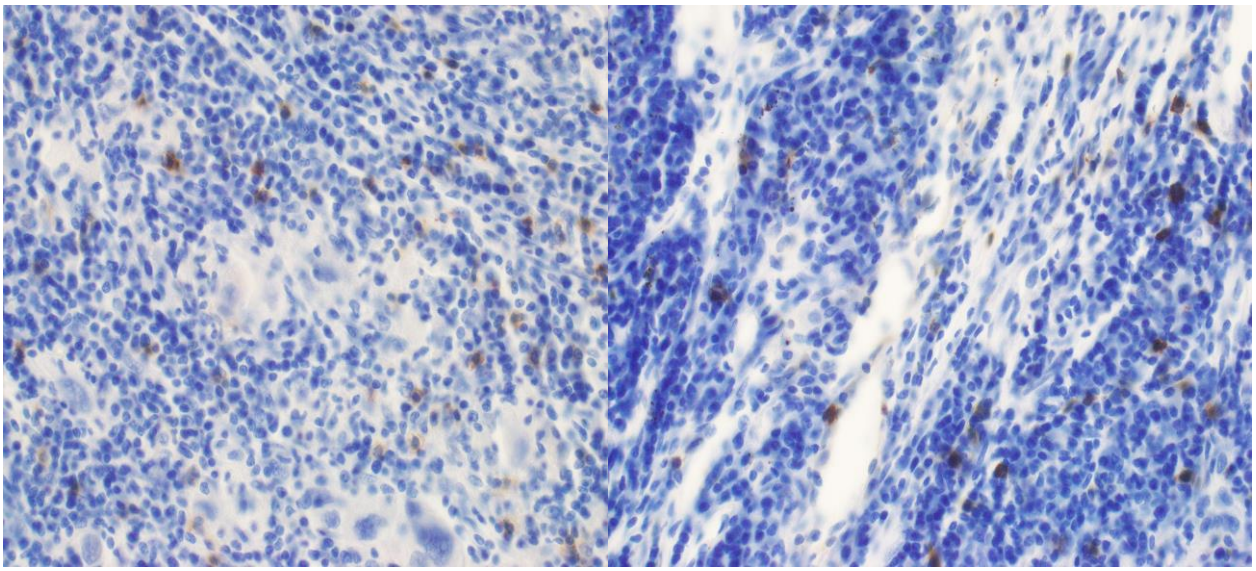

(A) (B)

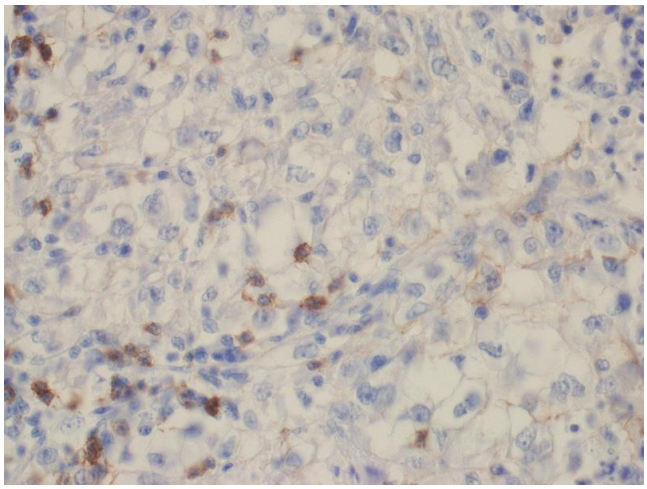

(C)

Fig. 5: Representative pictures of the immune cell infiltration in the primary ccRCC showing the CD56-positive cell infiltration intratumoral (A) peritumoral (B) and in the distant metastasis (C) (x200 magnification).

CD56 antibodies stained the CD56 positive immune cells, but in some cases, CD56 revealed a membranous positivity in the tumor tissue itself, especially at the invasive margin (Fig. 6).

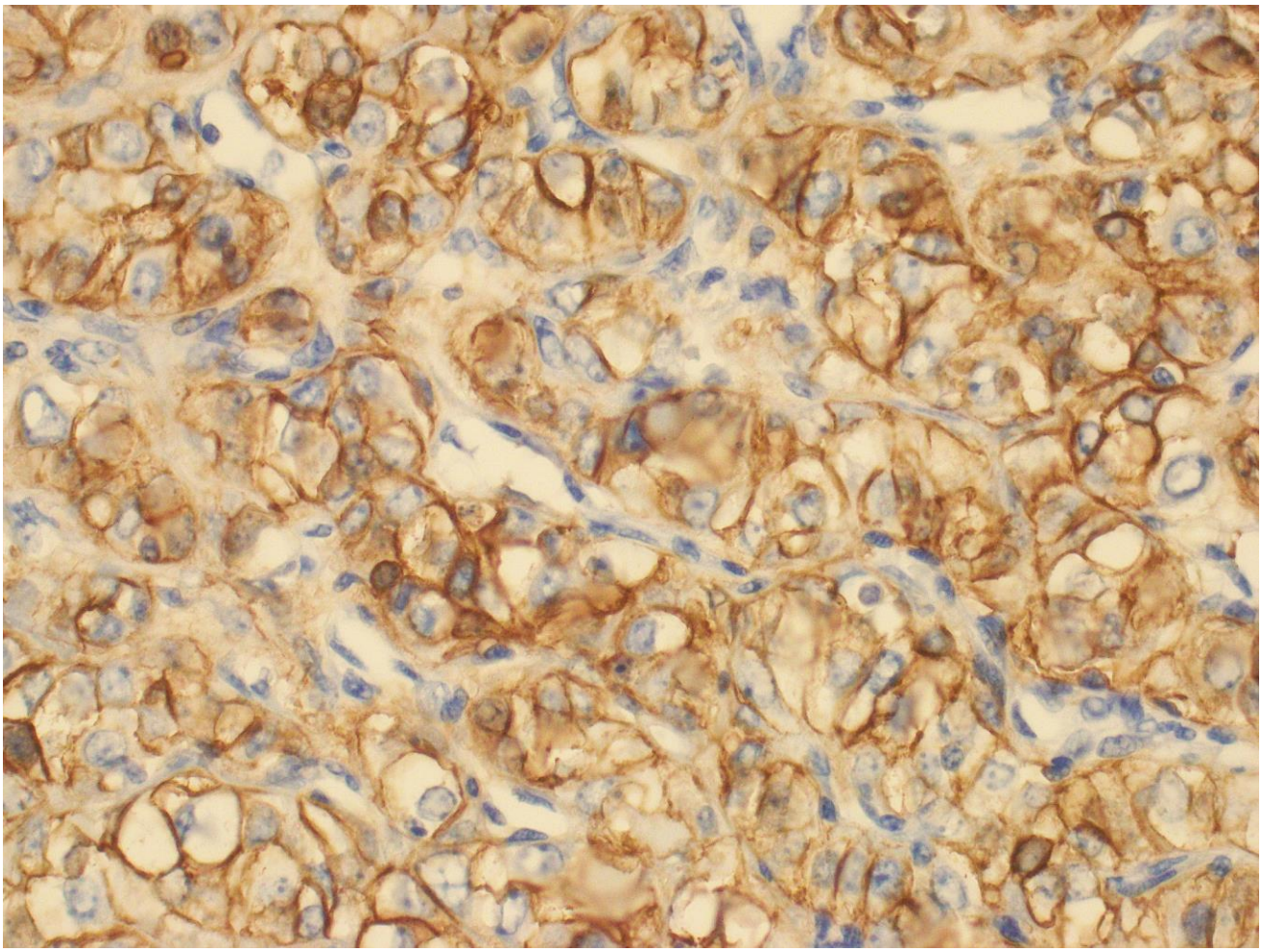

Fig. 6: Representative pictures of CD56-positive tumor cells primary in ccRCC (x400 magnification).

3.1.6. Infiltration of CD68-positive machrophages in ccRCC

CD68 cells revealed an average intratumoral infiltration of 32.6 cells/HPF with a range between 12 and 89 cells/HPF. The mean value for the peritumoral infiltration was 23.4 cells/HPF, the range was between 0.8 and 54 cells/HPF (Fig 7).

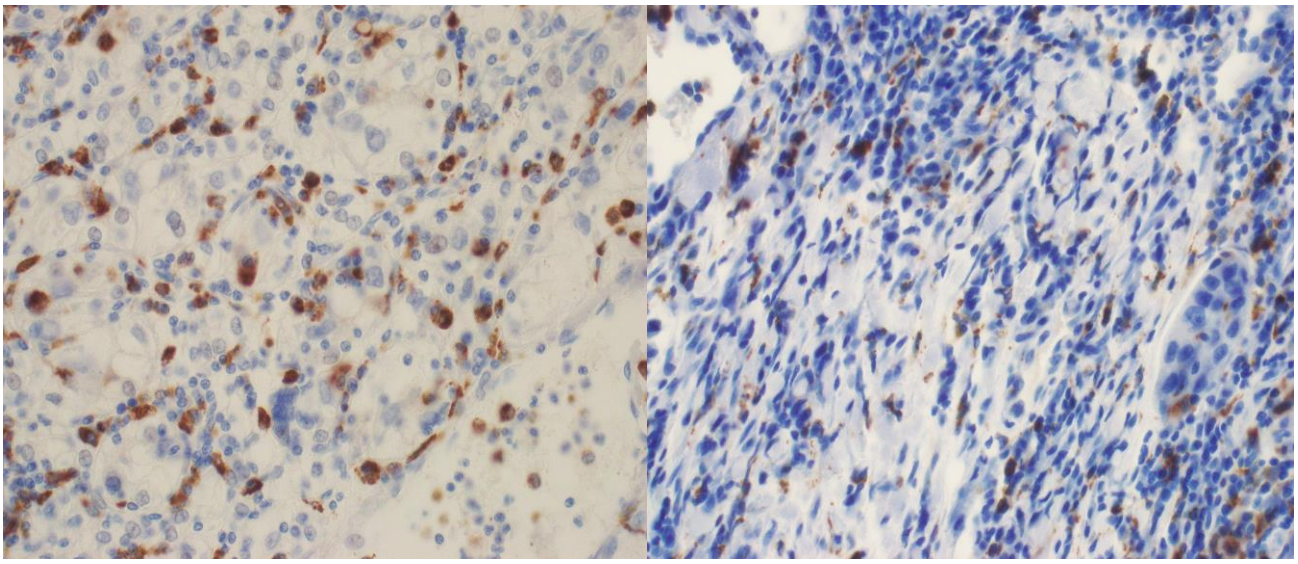

(A) (B)

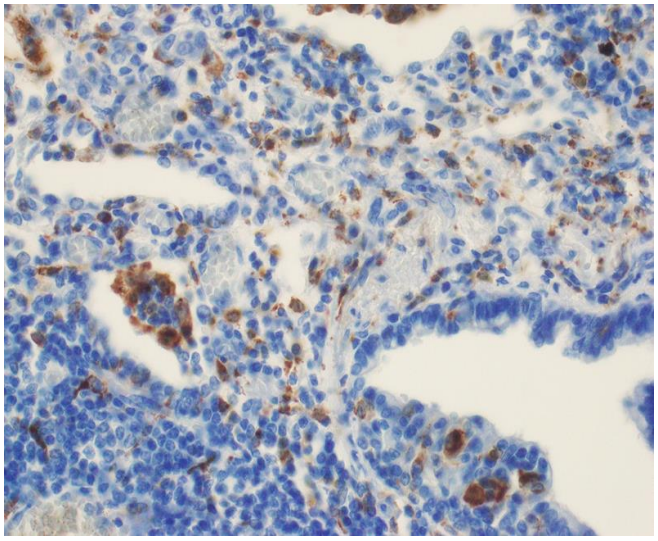

(C)

Fig. 7: Representative pictures of the CD68-positive cell infiltration in the primary ccRCC intratumoral (A) peritumoral (B) and in the distant metastasis (C) (x200 magnification).

3.1.7. Infiltration of CD103-positive cells in ccRCC

CD103 positive cells were observed in all tumors and metastases. The CD103 infiltration of the metastases (mean 38.1 cells/HPF) was significantly more abundant than the primary tumor (mean 15.96 cells/HPF) (Fig 8).

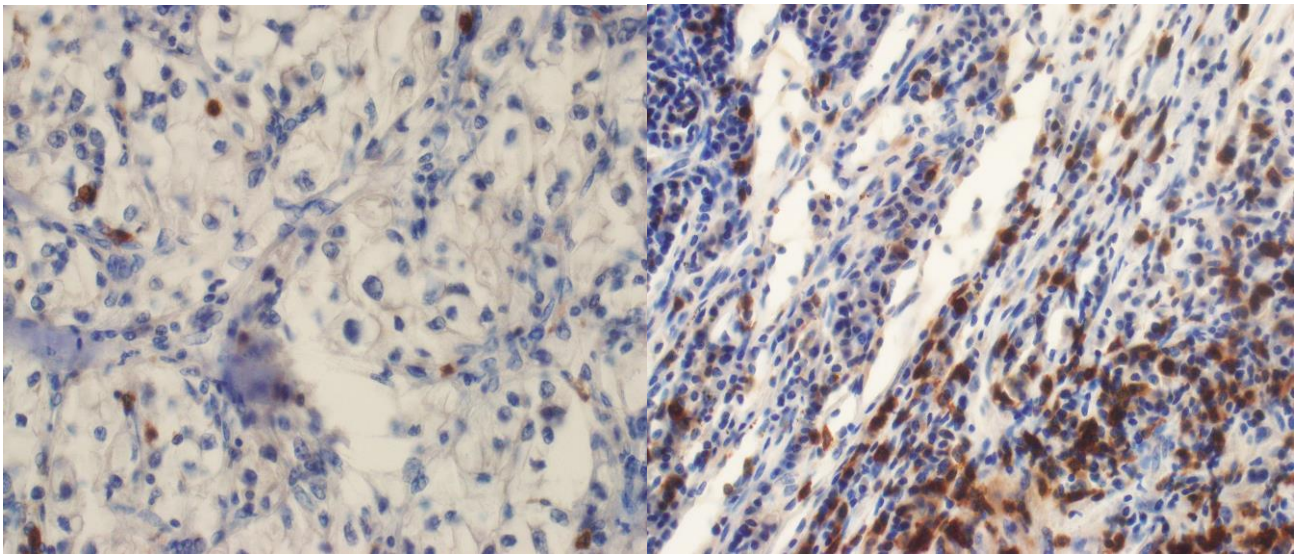

(A) (B)

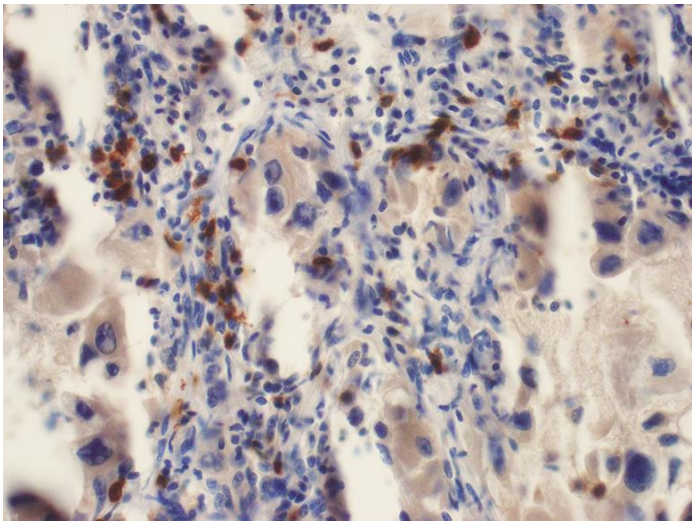

(C)

Fig.8: Representative pictures of the CD103-positive cell infiltration in the primary ccRCC intratumoral (A) and peritumoral (B) and in the distant metastasis (C) (x200 magnification).

3.2 Comparison of the amount of immune cell infiltrate with clinico-pathological parameters in primary ccRCC

3.2.1 Analysis of the amount of immune cell Infiltration in different pT-stages of primary ccRCC

Regarding the pT stage we split up the patients in two groups: one group for the pT1 and pT2 stages (organ confined tumors) and the other group containing pT3 and pT4 stages (organ non-confined tumors) stages. There were no statistical differences between the two groups (Tab. 3).

Tab. 3: Comparison of the tumor-infiltrating immune cells according to the T-stage.

Intratumoral immune cell infiltration				Peritumoral immune cell infiltraion			
Immune cell type	T1 & T2	T3 & T4	P-value	Immune cell type	T1 & T2	T3 & T4	P-value
CD3	72.5	61.0	0.3	CD3	107.4	104.9	0.4
CD4	36.4	27.1	0.1	CD4	51.2	57.9	0.2
CD8	48.9	34.6	0.2	CD8	60.0	57.5	0.4
CD20	3.8	1.9	0.07	CD20	23.7	30	0.2
CD56	4.4	3.9	0.4	CD56	7.8	5.2	0.1
CD68	33.2	32.2	0.4	CD68	23.9	23.8	0.5
CD103	16.1	15.8	0.5	CD103	22.6	25.7	0.3

3.2.2 Analysis of the amount of immune cell infiltration in different pN-stages of primary ccRCC

There were significant statistical differences in the immune cell infiltration between the N0 (without lymph node metastases) and the N1 (with lymph node metastases) patients. The patients without lymph node metastases showed higher intratumoral infiltrations for the cells CD4, CD8, and CD20 (Tab. 4 and Fig. 9).

Tab. 4: Comparison of the tumor-infiltrating immune cells according to the lymph node infiltration status.

Intratumoral immune cell infiltration				Peritumoral immune cell infiltration			
Immune cell Type	N0	N1	P-value	Immune cell type	N0	N1	P- value
CD3	83.7	58	0.3	CD3	113.8	99.2	0.3
CD4	43.1	12.2	**0.02**	CD4	58.1	68.3	0.3
CD8	59.1	9.8	**0.009**	CD8	64.8	50.6	0.2
CD20	2.2	0.24	**0.001**	CD20	30.6	37	0.3
CD56	4.1	1.68	0.054	CD56	4.7	7.7	0.2
CD68	36	28.2	0.09	CD68	23.5	23.7	0.4
CD103	25.2	15.8	0.1	CD103	25.1	25.1	0.49

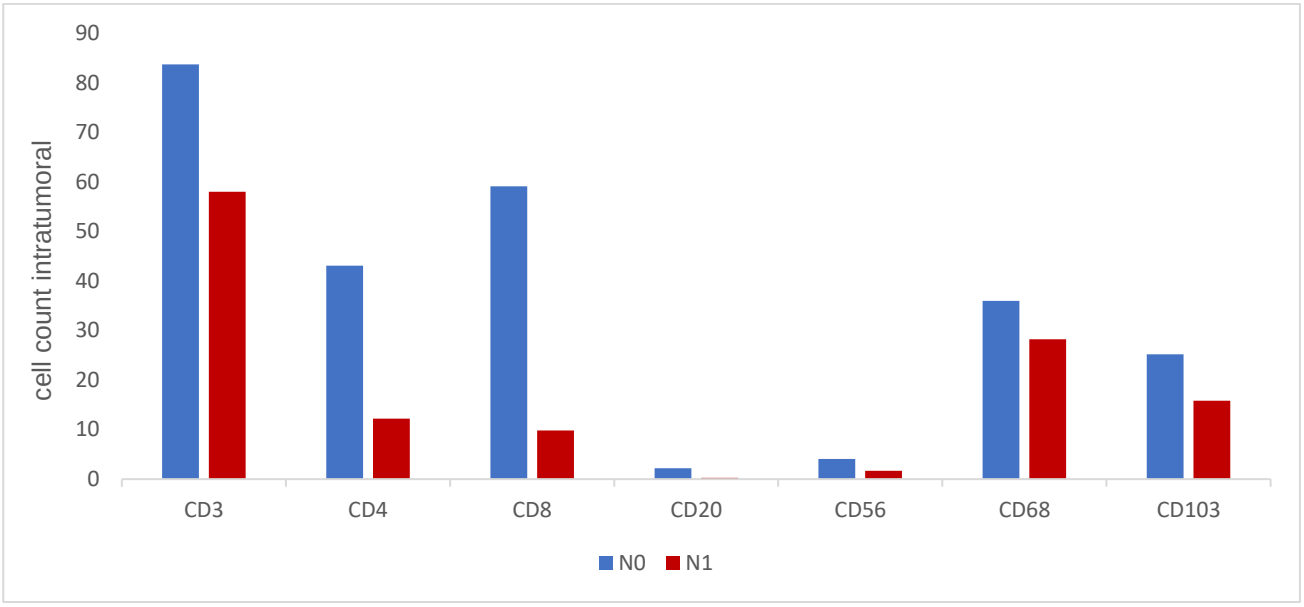

(A)

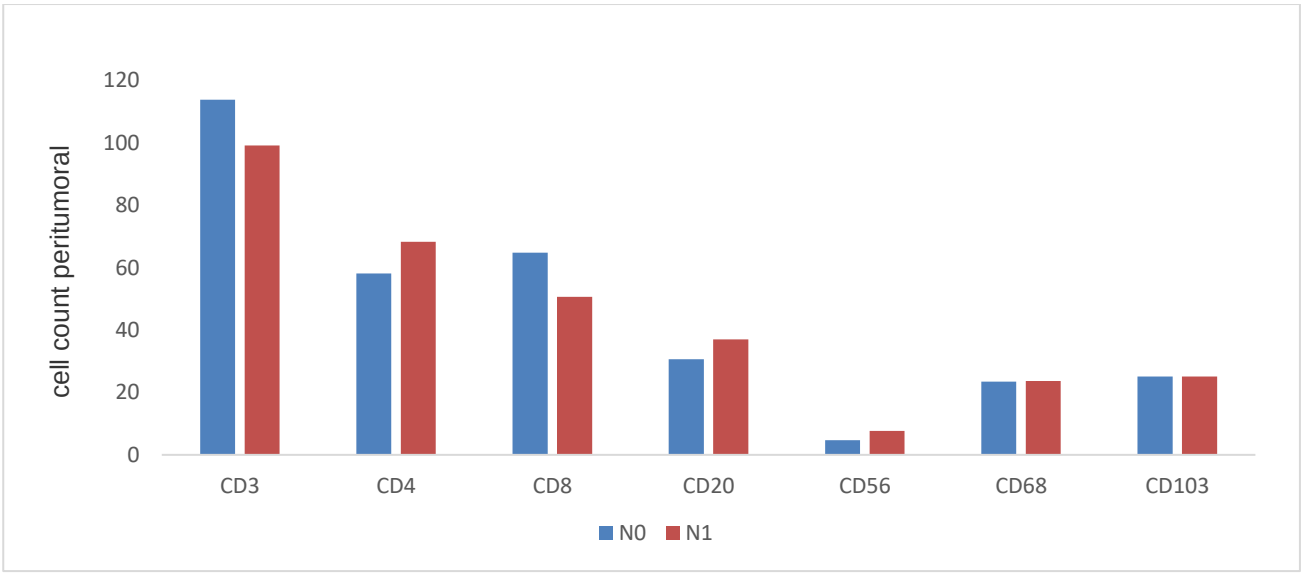

(B)

Fig. 9: Immune cell infiltration according to the lymph node status intratumoral (A) and peritumoral (B).

3.2.3 Comparison of the immune cell infiltrate in tumors without and with distant metastases

There were no significant differences in the Immune cell infiltration intratumorally between the patients with distant metastases (M1) and those without distant metastases (M0). Peritumoral immune cell infiltration was also without significant differences, except for the CD3 cells, which were significantly richer in the M1 patients (Tab. 5 and Fig. 10).

Tab. 5: Comparison of the tumor-infiltrating immune cells between patients with (M1) and without (M0) distant metastases.

Immune cell type	M1 intratumoral	M0 intratumoral	P-value	M1 peritumoral	M0 peritumoral	P-value
CD3	51.6	82.6	*0.07*	116.2	93.2	**0.03**
CD4	24.4	38.9	0.1	61.9	48	0.06
CD8	29.1	52	*0.06*	60.9	55	0.3
CD20	2.8	2.6	0.4	28.2	26	0.4
CD56	3.8	4.5	0.2	6.1	6.7	0.1
CD68	30.9	21.5	0.1	25.5	35	0.2
CD103	15.7	16.2	0.5	24.9	23.7	0.4

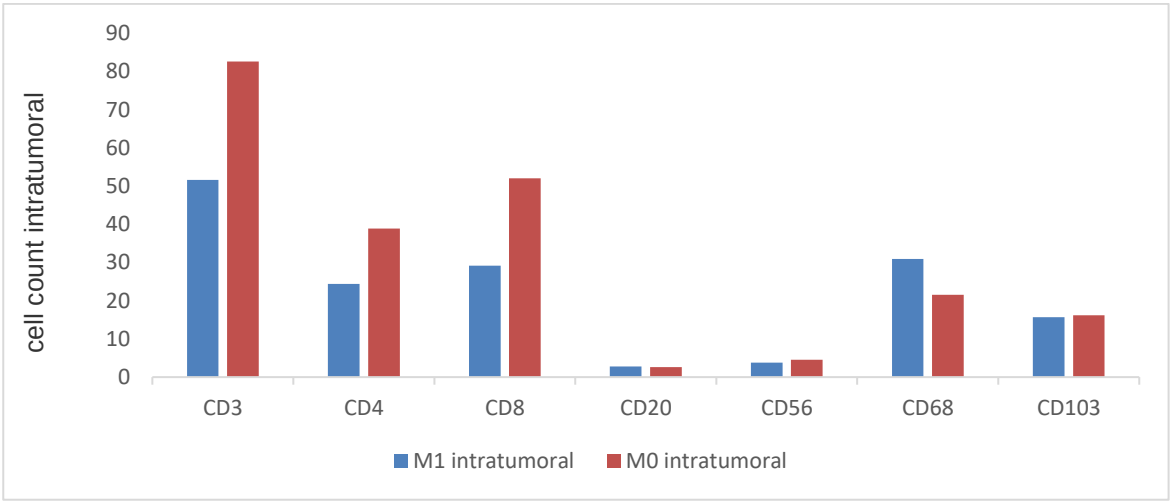

(A)

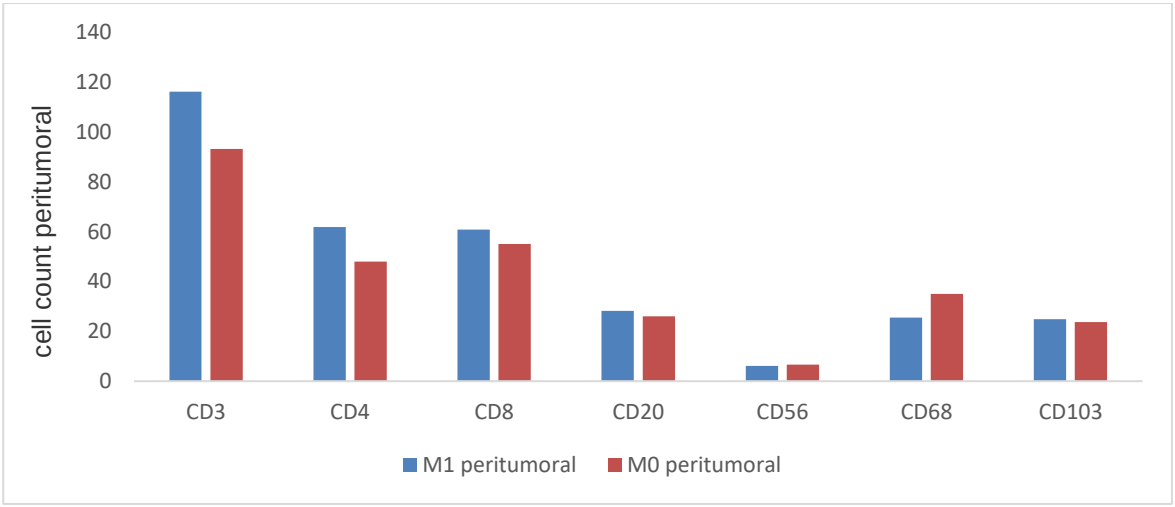

(B)

Fig. 10: Comparison of the tumor-infiltrating immune cells between patients with (A) and without distant metastases (B).

3.2.4. Effect of lymphovascular invasion on the immune cell infiltration

We wanted to know whether the lymphovascular invasion LVI could affect the immune infiltration, and therefore we calculated the immune cell infiltration for those with lymphovascular invasion LV1 and for those without lymphovascular invasion LV0. There was no statistical variation in the intratumoral immune cell infiltration. For the peritumoral immune

cell infiltration the CD56 were significantly more abundant in the LV0 tumors (Tab. 6 and Fig. 11).

Tab. 6: Comparison of the tumor-infiltrating immune cells between the tumors with and without lymphovascular invasion.

Intratumoral immune cell infiltration				Peritumoral immune cell infiltration			
Immune cell type	LV1	LV0	P-value	Immune cell type	LV1	LV0	P-value
CD3	67.3	53.8	0.3	CD3	105.6	100.4	0.2
CD4	30.7	29.9	0.4	CD4	59.18	49.3	0.1
CD8	42.3	35.5	0.3	CD8	58.8	50.8	0.1
CD20	2.1	3.8	0.1	CD20	31.7	19.1	0.054
CD56	4.2	4	0.4	CD56	4.1	8.4	**0.03**
CD68	31.7	32.9	0.4	CD68	22.4	25.1	0.2
CD103	16.4	15.9	0.4	CD103	24.5	20.7	0.2

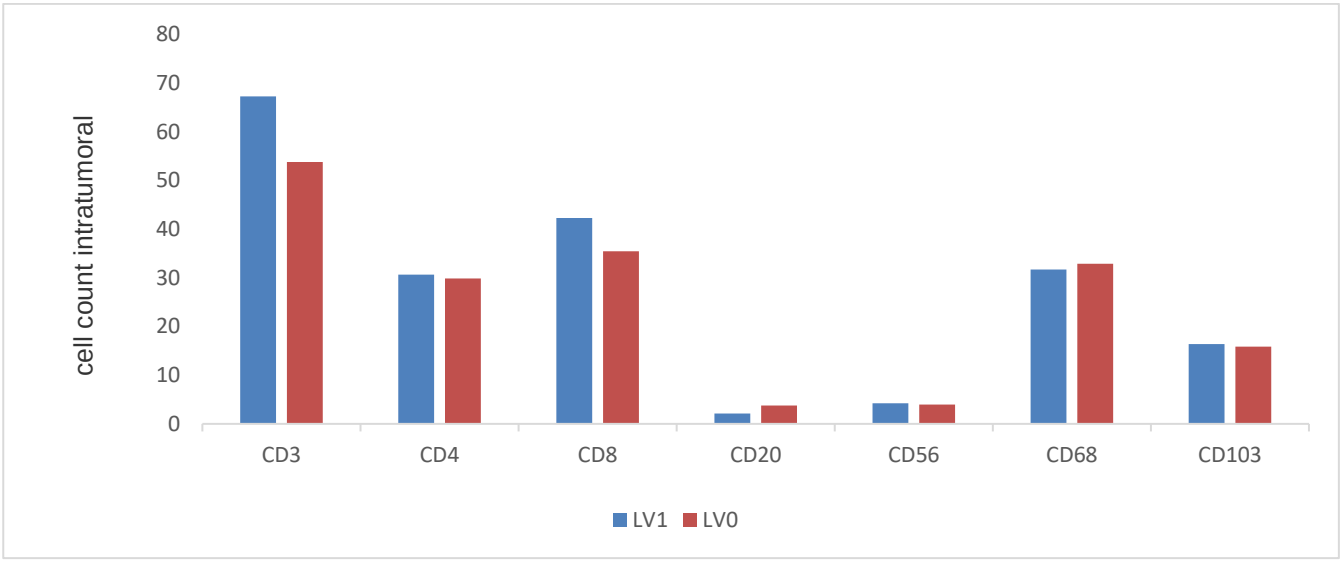

(A)

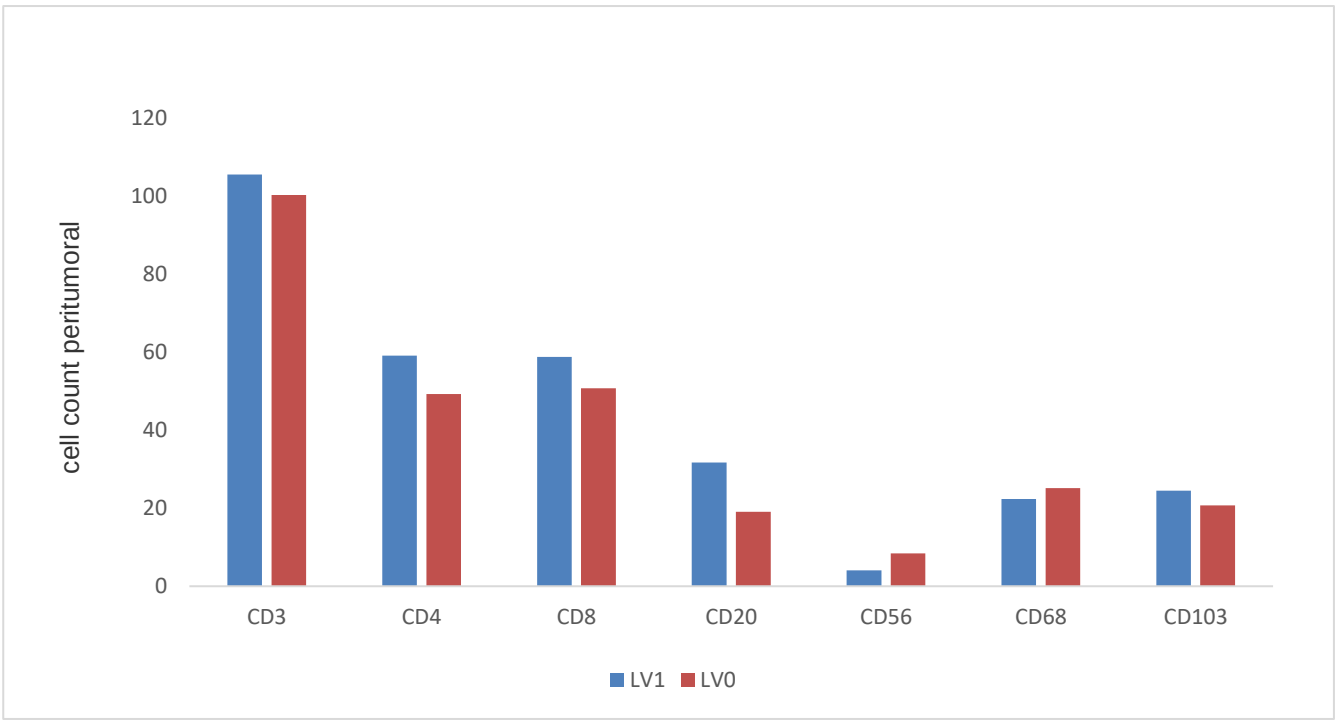

(B)

Fig. 11: Comparison of the immune cell infiltration between the LV1 and LV0 status for the intratumoral (A) and the peritumoral (B) infiltration.

3.2.5 Characterization of the immune cell infiltrate according to Fuhrman tumor grading in primary ccRCC

After having divided the patients into two groups according to the differentiation of the tumor (well-differentiated tumors comprising the G1 and G2 tumors and poorly-differentiated tumors comprising G3 and G4 tumors) we found that the CD4 and CD8 cell number in the tumor tissue was higher in the well differentiated tumors compared with the poorly differentiated ones.

For the peritumoral immune cell infiltration the CD103-positive cells revealed higher peritumoral infiltration in the well differentiated tumors than in the poorly differentiated ones. The other subtypes showed no statistic significant differences between well- and poorly-differentiated tumors (Tab. 7 and 8, Fig. 12).

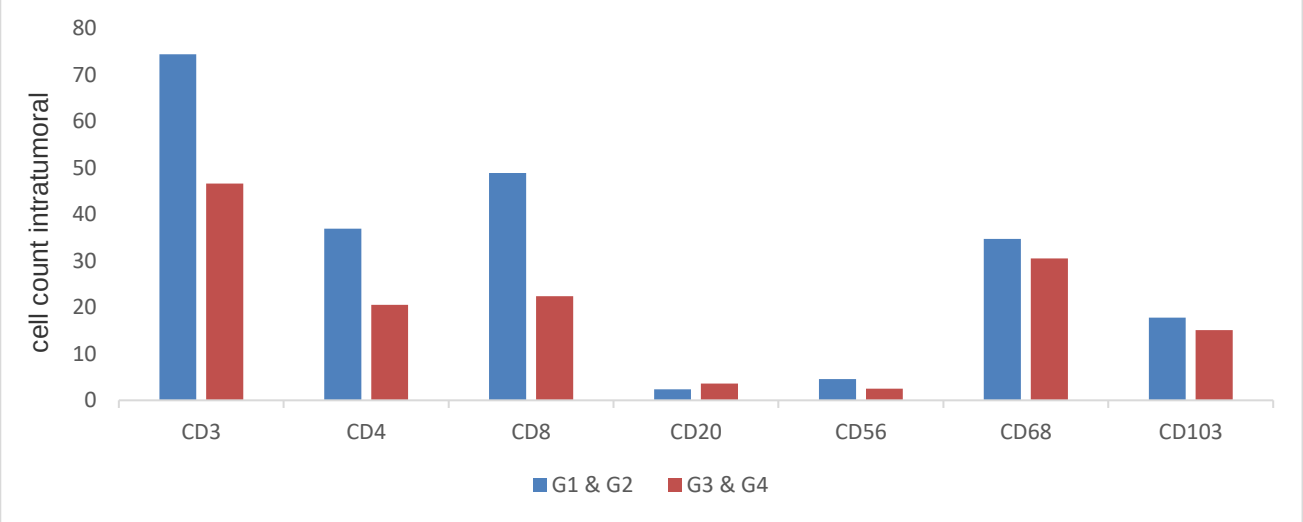

(A)

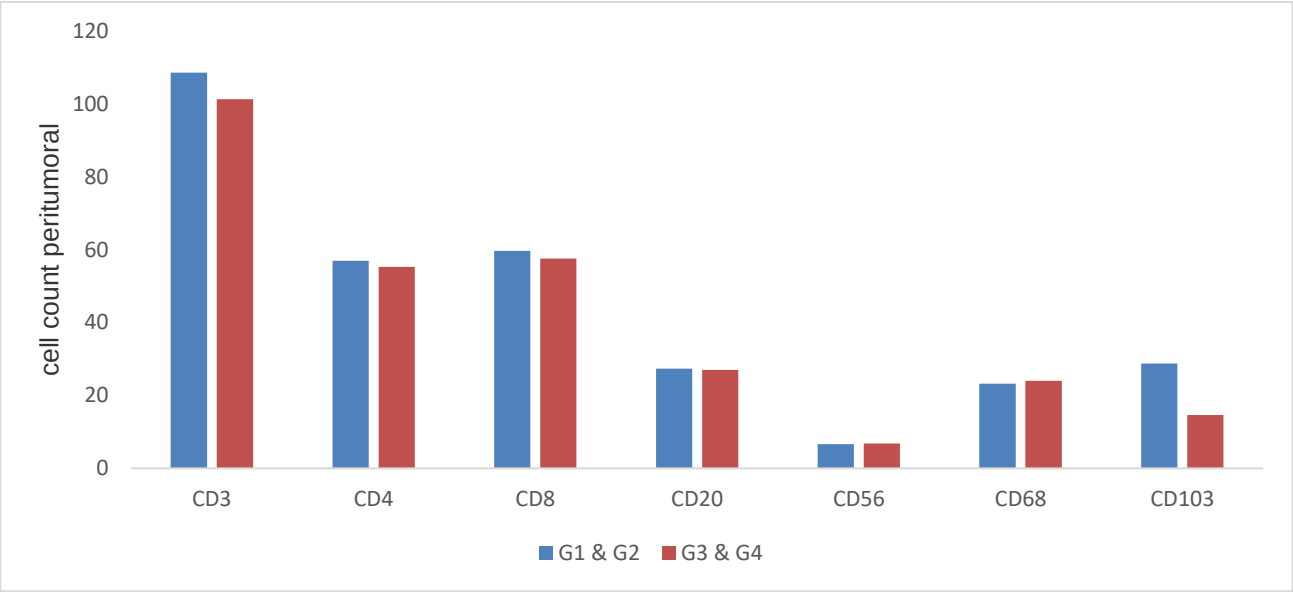

(B)

Fig. 12: Comparison of the intratumoral (A) and peritumoral (B) immune cell infiltration between the well differentiated and poorly-differentiated tumors.

Tab. 7: Comparison of the intratumoral immune cells infiltration between the well-differentiated (G1 and G2) and the poorly-differentiated tumors (G3 and G4).

Immune cell Type	G1 & G2	G3 & G4	P-value
CD3	74.4	46.6	*0.06*
CD4	36.9	20.56	**0.03**
CD8	48.91	22.4	**0.02**
CD20	2.4	3.6	0.26
CD56	4.6	2.5	*0.07*
CD68	34.7	30.5	0.18
CD103	17.8	15.1	0.31

Tab. 8: Comparison of the peritumoral immune cell infltration between the well-differentiated (G1 and G2) and poorly-differentiated tumors (G3 and G4).

immune celll type	G1 & G2	G3 & G4	P-value
CD3	108.6	101.3	0.27
CD4	56.94	55.32	0.43
CD8	59.7	57.58	0.38
CD20	27.4	27	0.47
CD56	6.6	6.8	0.46
CD68	23.2	24	0.37
CD103	28.8	14.6	**0.001**

We also compared the CD4/CD8 ratio between the well-differentiated (G1 and G2) and poorly-differentiated ones (G3 and G4) and noticed no significant differences regarding this ratio.

Tab. 9: Ratio of the CD4/CD8 for the well- (G1 and G2) and the poorly-differentiated tumors (G3 and G4).

	G1 and G2 tumors	G3 and G4 tumors	p-value
CD4/CD8 ratio for the intratumoral Infiltration	1.04	1.32	0.2
CD4/CD8 ratio for the peritumoral infiltration	0.91	1.08	0.1

3.3. Immune cell infiltrate in primary tumor versus distant metastases

After having compared the immune cell infiltration between the primary tumor and the distant metastases, we found significant differences in the CD103-positive cell infiltration, which were richer in the tumor metastases than in the primary tumor (Tab. 10 and Fig. 13). By contrast, the CD68 cell infiltration was significantly higher in the primary tumor than in the metastases. All other investigated subtypes showed no significant differences between the primary tumor and the associated distant metastases.

Tab. 10: Comparison of the tumor-infiltrating immune cells between the primary tumors and the distant metastases.

Immune cell type	Primay tumor	Metastases	P-value
CD3	82.6	54.4	0.2
CD4	38.9	24.4	0.2
CD8	52.6	42.6	0.4
CD20	2.6	2.6	0.4
CD56	4.5	5.6	0.3
CD68	35	24.4	**0.02**
CD103	16.2	38.1	**0.01**

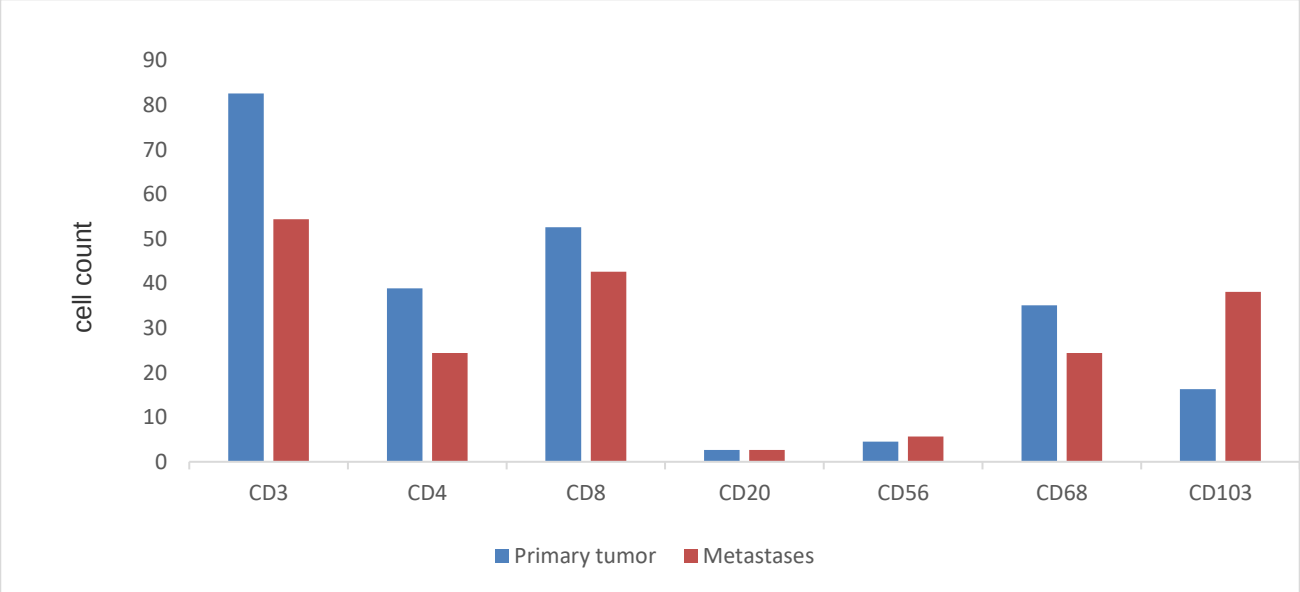

Fig. 13: Comparison of the tumor-infiltrating immune cells between the primary tumor and distant metastases.

3.4. Differences in immune cell infiltration between different sites of metastases

Subsequently, we compared the immune infiltration between the lung, bone and lymph nodes metastases. Different sites of distant metastases showed different immune cell infiltration rates, whereby the lung metastases showed the most abundant immune cell infiltration (Tab. 11 and Fig. 14). By contrast bone tissue revealed the lowest immune cell infiltration, with the exception of the CD68 cells.

Tab. 11: Comparison of the tumor-infiltrating immune cells between the lung, lymph node and bone metastases.

Immune cell type	lung met. (n=6)	lymph node met. (n=4)	bone met. (n=7)	p value lung vs. bone met.	p value lung vs. lymph node met.	p value bone vs. lymph node met.
CD3	98	50	18.8	**0.01**	*0.09*	0.1
CD4	42.4	11.53	9.2	**0.02**	**0.04**	0.4
CD8	82.61	41.2	16.9	*0.056*	0.1	0.1
CD20	4.31	3.65	1.8	0.1	0.4	0.2
CD56	13.6	4.05	1.73	0.1	0.1	0.1
CD68	19.88	31.2	19.6	0.4	0.1	0.1
CD103	62.33	38.05	14.9	**0.04**	0.1	0.1

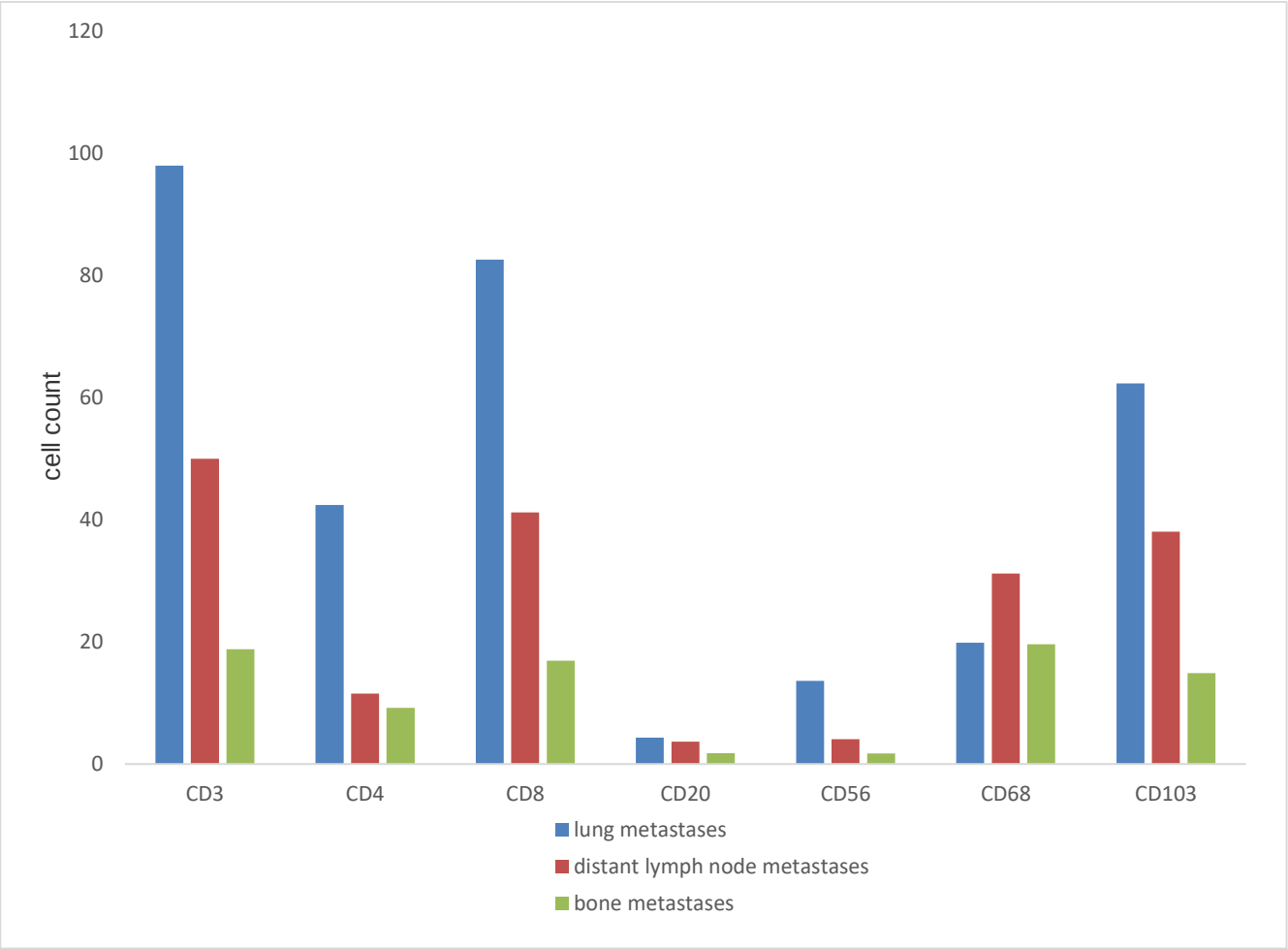

Fig. 14: Comparison of the tumor-infiltrating immune cells between the lung, lymph node and bone metastases.

CD3, CD4 and CD103 had a significantly higher count in the lung metastases compared with the bone metastases. When compared with lymph node metastases, the significance was only present for the CD4 cells.

3.5. CD56 positive tumors

We used the CD56 staining in this study to detect the CD56+ lymphocytes. CD56 – also called neural cell adhesion molecule (NCAM) – is used in some cases as a marker for neuroendocrine differentiation. In this study, 26% of primary ccRCC were positive for CD56 (13/50 cases), from which nine cases of CD56 positive tumors showed distant metastases (M1) and only four cases of CD56 positive tumors had no distant metastases (M0) (Tab. 12).

Tab. 12: Proportion of the CD56 positive tumors in this study

M stage	Number of CD56 positive tumors
All patients	13 (26%)
M1 patients	9 (32%)
M0 patients	4 (18%)

Interestingly, a comparison of the tumor-infiltrating immune cells between the CD56-positive and CD56-negative tumors showed significant differences for the lymphocyte infiltration, as the intratumoral cell count for CD3, CD4, CD8 and CD20 cells was significantly lower in the CD56 positive tumors (Tab. 13 and 14, Fig. 15).

There was no association of the CD56 expression with the tumor grade nor with the tumor size.

Tab. 13: Comparison of the intratumoral Immune cell infiltration between the CD56- tumors and CD56+ tumors.

Immune cell type	Number of the intratumoral immune cells in CD56- tumors	Number of the intratumoral immune cells in CD56+ tumors	P-value
CD3	92.3	24.1	**0.001**
CD4	44.8	13.7	**0.01**
CD8	60.6	9.9	**0.008**
CD20	2.7	2	**0.001**
CD56	4.88	2.2	0.4
CD68	31.5	49	0.09
CD103	16.6	14.5	0.1

Tab. 14: Comparison of the peritumoral immune cell infiltration between the CD56-tumors and CD56+ tumors

Immune cell type	Number of the peritumoral immune cells in CD56- tumors	Number of the peritumoral immune cells in CD56+ tumors	P-value
CD3	104.7	109.5	0.3
CD4	43.4	67.2	0.4
CD8	51.7	77	0.2
CD20	19.1	59.8	0.2
CD56	6.6	7.1	0.4
CD68	20.1	27	0.2
CD103	21.1	34.2	0.4

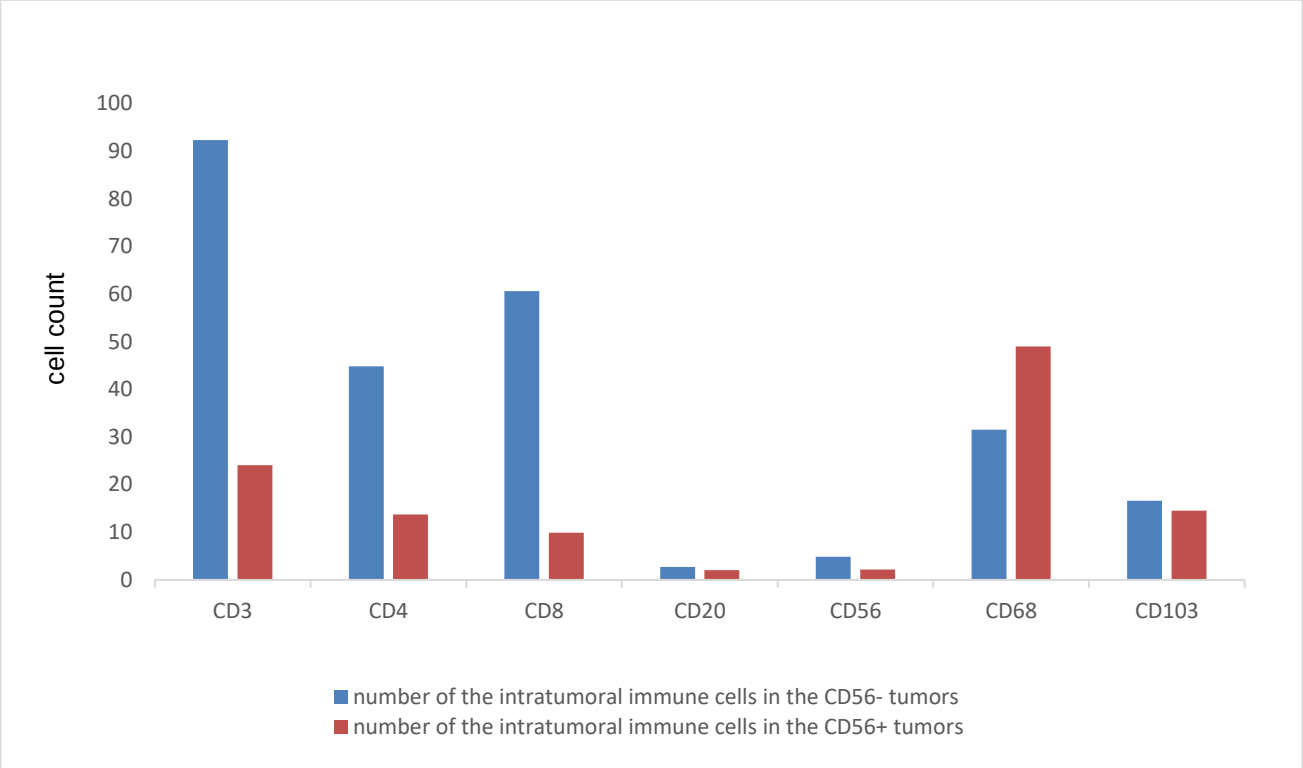

Fig. 15: Comparison of the intratumoral immune cell infiltration between the CD56+ and CD56- RCC.

3.6. Correlation analysis between different subtypes of immune cells in ccRCC

Some subtypes of immune cells show strong correlation with other subtypes. The CD3 cells showed a strong correlation with the CD4 and CD8 cells. CD103 revealed a moderate correlation with the CD3-, CD4- and CD8-positive cells. The CD56-positive immune cells showed a strong correlation with the CD8-positive T-lymphocytes in the metastases but not in the primary tumor (Tab. 15 and 16, Fig. 16 and 17).

Tab. 15: Pearson correlation analysis between the different tumor-infiltrating immune cells for the intratumoral immune cell infiltration in the primary tumor.

Intratumoral Immune cell infiltration in primary tumors	CD3	CD4	CD8	CD20	CD56	CD68	CD103
CD3		0.8	0.9	0.1	0.2	0.05	0.6
CD4	0.8		0.8	0.2	0.4	-0.06	0.5
CD8	0.9	0.8		0.2	0.2	0.03	0.6
CD20	0.1	0.2	0.2		-0.003	0.1	0.2
CD56	0.2	0.4	0.2	-0.003		-0.003	0.2
CD68	0.05	-0.06	0.03	0.1	-0.003		0.05
CD103	0.6	0.5	0.6	0.2	0.2	0.05	

Tab. 16: Pearson correlation analysis between the different tumor-infiltrating immune cells for the immune cell infiltration in the metastases.

Immune cell infiltration in the metastases	CD3	CD4	CD8	CD20	CD56	CD68	CD103
CD3		0.7	0.8	0.7	0.6	0.3	0.6
CD4	0.7		0.3	0.3	0.09	0.04	0.1
CD8	0.8	0.3		0.7	0.8	0.2	0.7
CD20	0.7	0.3	0.7		0.5	0.06	0.7
CD56	0.6	0.09	0.8	0.5		0.1	0.6
CD68	0.3	0.04	0.2	0.06	0.1		0.03
CD103	0.6	0.1	0.7	0.7	0.6	0.03	

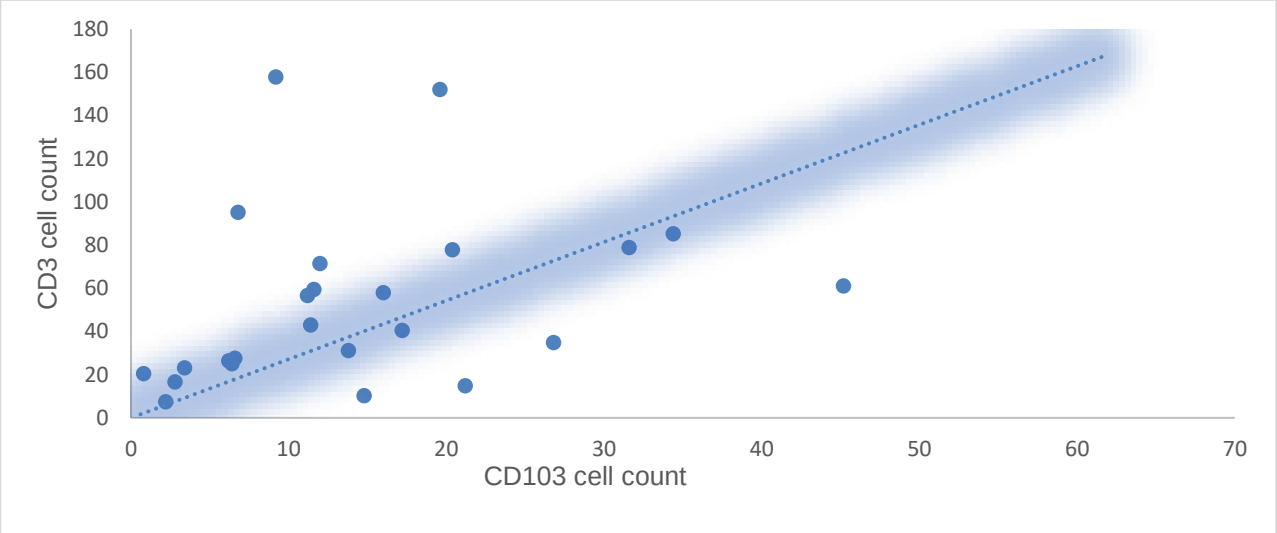
CD3 cell count
CD103 cell count
0
20
40
60
80
100
120
140
160
180
0
10
20
30
40
50
60
70

(A)

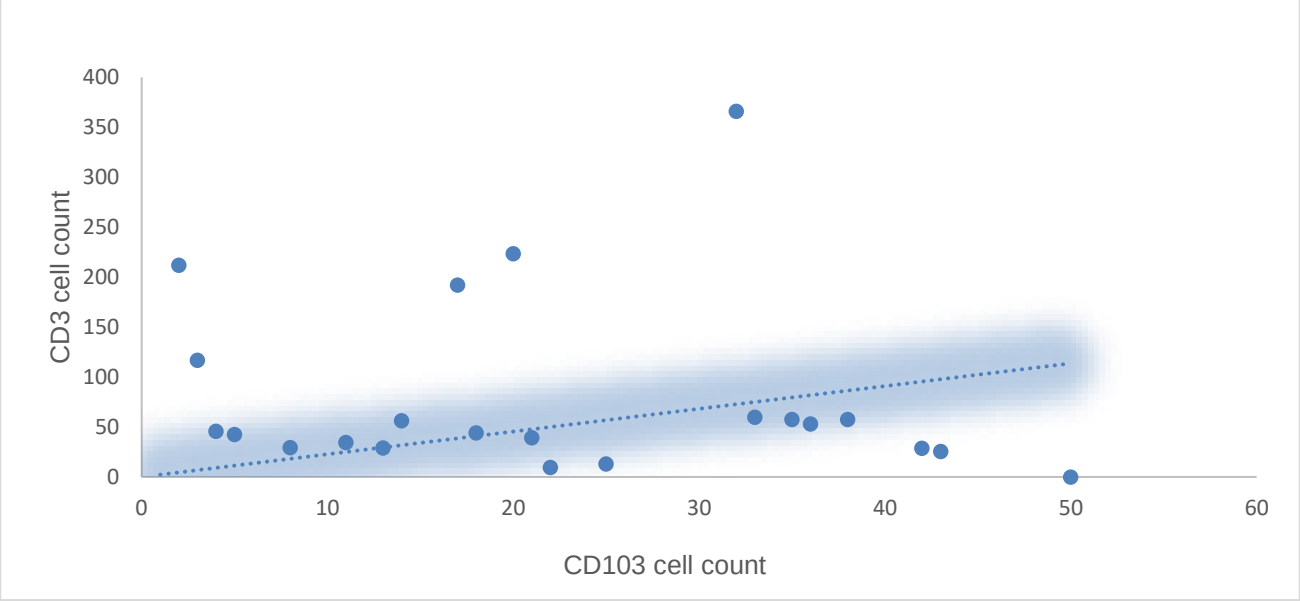
CD3 cell count
CD103 cell count
0
50
100
150
200
250
300
350
400
0
10
20
30
40
50
60

(B)

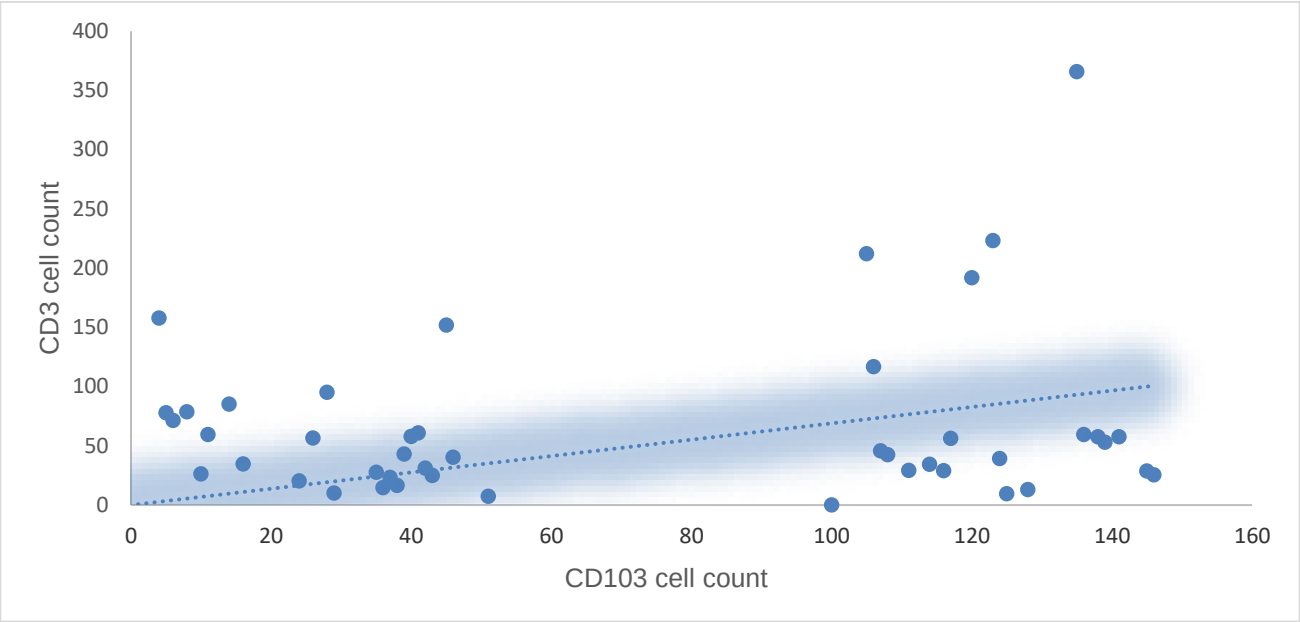

(C)

Fig. 16: Pearson correlation between the CD103 infiltration and the CD3 cells in the M1 patient group (A) and the M0 patient group (B) and for all groups (C).

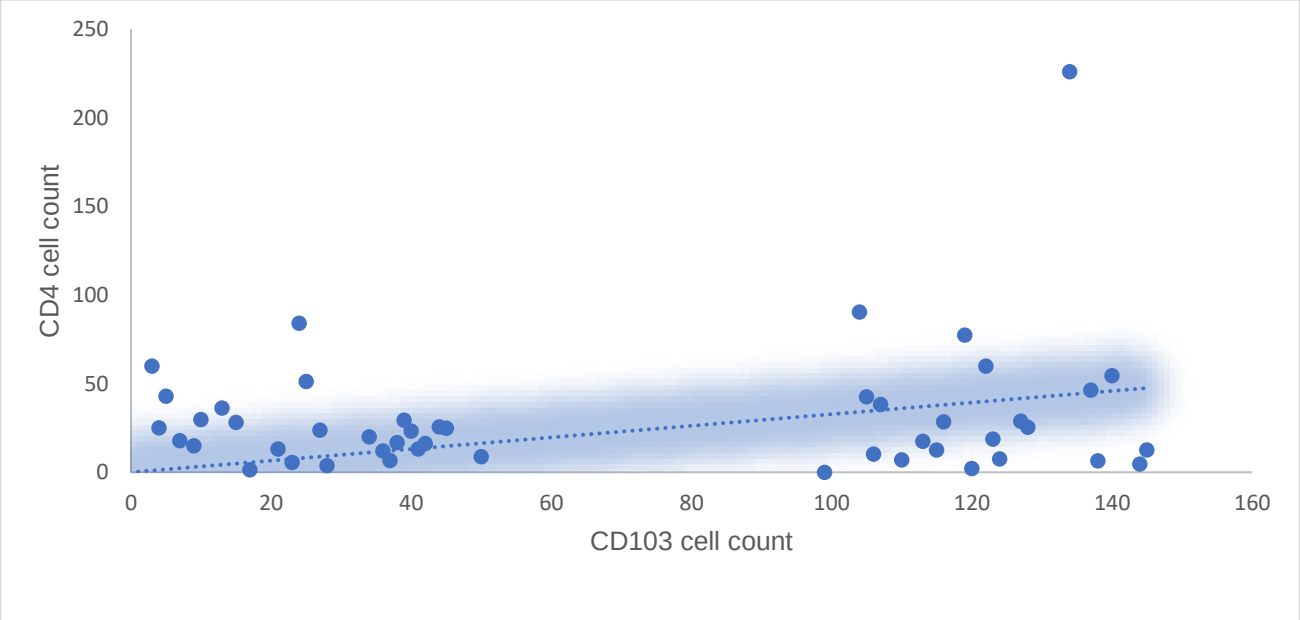

(A)

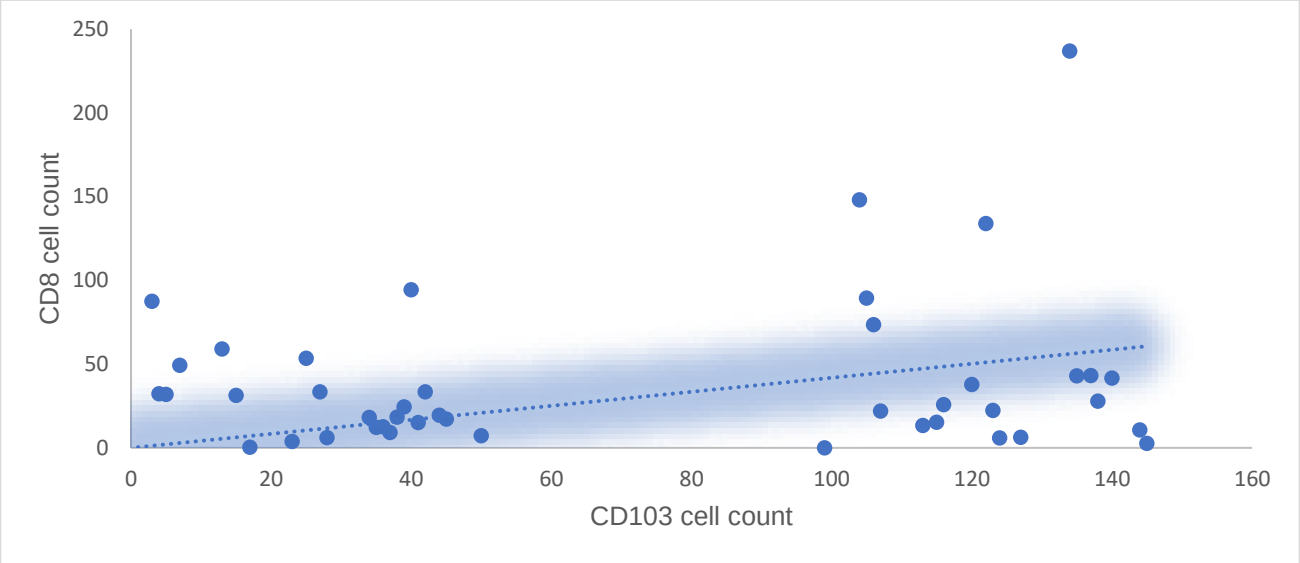

(B)

Fig. 17: Pearson correlation between the CD103 infiltration and the CD4 cells (A) and the CD8 cells (B).

3.7. Immune cell ratio intratumoral/peritumoral in ccRCC

3.7.1. Immune cell ratio intratumoral/peritumoral in ccRCC according to tumor grade

We also wanted to investigate the ability of the immune cells to infiltrate the tumor tissue by determining the ratio of the intratumoral to the peritumoral immune cell infiltration for each immune cell subtype and case. We then compared the ratios of each subtype according to the grade of tumor differentiation using the Mann–Whitney U test.

Interestingly CD8-positive lymphocytes showed a significantly stronger tumor infiltration ability in the well-differentiated tumors compared to the poorly-differentiated ones (Tab. 17).

Tab. 17: Ratio of the intratumoral/peritumoral immune cell infiltration for the well- (G1 and G2) and the poorly-differentiated tumors (G3 and G4).

Immune cell type	G1 & G2 intratumoral/ peritumoral infiltration ratio	G3 and G4 intratumoral/ peritumoral infiltration ration	P-value
CD3	0.82	0.43	0.2
CD4	0.84	0.42	0.2
CD8	0.9	0.36	**0.01**
CD20	0.3	0.19	0.6
CD56	1.23	0.68	0.4
CD68	1.86	1.66	0.9
CD103	0.73	1.06	0.1

3.7.2. Immune cell ratio intratumoral/peritumoral in ccRCC according to distant metastases

We also found interesting results after having compared this immune cell ratio between the primary tumors of patients with and without metastases. This ratio was significantly higher for the CD3-lymphocytes in the primary tumors of patients with metastases (Tab. 18).

Tab. 18: Ratio of the intratumoral/peritumoral immune cell infiltration for the primary tumors of M0 and M1 Patients.

Immune cell type	intratumoral/ peritumoral infiltration ratio in the primary tumors of M0 patients	intratumoral/ peritumoral infiltration ratio in the primary tumors of M1 patients	P value
CD3	0.45	1.02	**0.049**
CD4	0.49	0.92	0.1
CD8	0.47	0.97	0.1
CD20	0.31	0.23	0.1
CD56	0.86	1.40	0.4
CD68	1.72	4.06	0.4
CD103	0.75	0.83	0.8

4. Discussion

The tumor microenvironment contains different types of cells like fibroblast, endothelial cells and several subtypes of immune cells. The tumor invasiveness is not only determined through properties of the cancer cells itself, but also through interaction with these the stromal cells (Kovaleva et al., 2016). Some of these immune cells could enhance the immunologic response against the tumor, while on the other hand other subtypes have an immunosuppressive function and therefore could promote tumor growth. Furthermore, the spatial architecture of the immune microenvironment could be a prognostic index in malignant tumors. (Selvi et al., 2020).

A comprehensive description of the immune cell infiltrate in malignant tumors could help to improve the treatment of these tumors, especially in immunotherapy.

4.1 T-Cell infiltration in ccRCC

We investigated the immune cell infiltration in primary ccRCC tumors and in paired distant metastases.

We first assessed the count of T-lymphocytes by immunohistochemistry for CD3, which showed an abundant infiltration intratumoral and peritumoral in ccRCC. This is in line with the data published by (Chevrier et al., 2017). The peritumoral CD3 infiltration was significantly higher in the primary tumors of the M1 cases compared to M0 cases, but intratumoral tumor infiltration did not follow the same trend. This supports previous data published by (Giraldo et al., 2015) who demonstrated that the accumulation of T-lymphocytes in ccRCC is correlated with poor prognosis.

The analysis of the relationship between immune cell infiltration and clinical-pathological characteristics of ccRCC showed no association between immune cell infiltration and tumor stage, but the tumor grading was observed to be inversely associated with different subtypes of T-lymphocytes (CD4+ and CD8+). By contrast, Baine et al., (2015) showed no associations

between the grade of differentiation and the infiltration of CD4+ and CD8+ T-lymphocytes in the RCC.

In our study, there was no statistical difference in the intratumoral CD8 infiltration in the primary tumors and the metastases. Nevertheless the study by (Baine et al., 2015) revealed a significantly more abundant CD8 infiltration in the primary tumors compared to the metastases.

However, this discrepancy between the studies could be attributed to the subtype of RCC, since our study included only ccRCC, but other studies like Baine et al. (2015) also included other subtypes of RCC. This also indicates that immunologic response in the case of ccRCC is different in compared to other subtypes of the RCC. Further studies in the immunology of the RCC should always consider the tumor subtype.

An explanation for the higher T-cell infiltration in the well-differentiated tumors compared to the poorly-differentiated ones in this study could be the abundant expression of tumor antigens in the well-differentiated tumors, so that after recognition of the antigens a proliferation of the T-lymphocytes cells occurs.

Another explanation could be the Warburg effect noticed in malignant tumors, especially in ccRCC. The lower pH value in the tumor could inhibit the proliferation of the lymphocytes. The anaerobic glycolysis is highly regulated in the cancer cells. Even in excess of oxygen, the cancer cells still produce energy via anaerobic glycolysis. This special metabolic phenomenon of the cancer cells is known as Warburg effect (Choi et al., 2013). Lactic acid is generated from pyruvate via the lactate dehydrogenase enzyme. The lactic acid is produced in large quantities in the cancer tissue leading to acidification of the cancer microenvironment. In the study by Wettersten et al. (2015) on the metabolic aspects of RCC, it was shown that poor differentiation of the RCC is associated with upregulated glycolysis and higher lactic acid production.

We assume that the lower number of T-Lymphocytes in the poorly-differentiated tumors could be attributed to the higher acidity within these tumors. A low pH value has been shown to have negative impacts on CTLs through several mechanisms; for example by reducing the

cytotoxicity of the CTLs, proliferation inhibition of the CTLs, promoting the CTLs apoptosis, decreasing IL-2 and IFN-γ production by CTLs, as well as reducing perforin and granzyme production of CTLs (Huber et al., 2017). Singer et al. (2011) could demonstrate that expression of the glucose transporter GLUT-1 was higher in the tumor cells of the RCC compared with normal cells. The expression of GLUT-1 in the ccRCC was also inversely correlated with tumor infiltration through CD8+ T-lymphocytes. Nonetheless, further studies concerning the immune cells in the RCC should not ignore the metabolic side of this tumor.

Regarding the ratio of CD4+/CD8+ lymphocytes, we noticed no significant differences between different tumor stages, grading or the presence of distant metastases. In the study by Bersanelli et al. (2019), the CD4/CD8 ratio was inversely related to the Fuhrman grade of the primary tumor of RCCs. This could be due to the small patient number included in our study.

4.2 CD20 positive cells in ccRCC

The role of the CD20 cells in tumor tissue remains unclear, since studies on the association of the CD20 infiltration with the clinical outcome have shown different results. It seems that different subpopulations of the CD20 cells can affect the tumor response differently.

In high grade ovarian cancer, it has been shown that there is a strong correlation between the density of B- and T-lymphocytes (Milne et al., 2009). Our study revealed a strong correlation between the CD20+ lymphocytes and the T-lymphocytes revealed by CD3+ CD8+ and CD103+ immunohistochemical expression in the metastases.

This correlation could be explained through the fact that the CD20+ lymphocytes can serve as APCs inducing the proliferation of the T-cells. Additionally, it has been previously shown that the CD20 cells can produce cytokines like C-C motif chemokine ligand 22 (CCL22), which lead to chemotactic migration of the T-cells (Ghadially et al., 2005). Interestingly the association between the B-cells and different subtypes of the T lymphocytes was found in the metastases but not in the primary renal tumor. This can indicate that the presentation of the tumor antigens is more advanced in the metastases than in the primary tumors.

Remarkably, our analysis showed a significant lower CD20 cells intratumorally in the patients with lymph node tumor infiltration. We assume that insufficient immune response in tumors with sparse CD20 infiltration is the reason for the higher incidence of lymph node metastases. It is possible that higher tumor infiltration by the B-cells slow down the development of lymph node metastases.

In our study, the number of intratumoral B-lymphocytes – identified as CD20+ cells – was inversely correlated with the occurrence of local lymph node metastases. Other studies published by Stenzel et al. (2019) showed an association between high amounts of intratumoral CD20+ lymphocytes and cancer-specific survival. Our collective is too small for a properly survival analysis, but our observations are in line with the study by Stenzl et al. (2019). Opposite to this, a further study published by (Sjöberg et al., 2018) demonstrated that high intratumoral infiltration by CD20+ lymphocytes correlated with a shorter overall survival in patients with ccRCC.

It should be noted that our study investigated the CD20 positivity, which considered as general marker for the B lymphocytes. Further studies are needed to reveal the role of the different types of the B-lymphocytes and their correlations to the clinicopathological parameters in RCC, since the CD20+ cells can enhance or suppress the immunological response depending on their subtype and its cytokine production.

Moreover, studies regarding the immunogenic subsets of the B-cells like the plasma cells (which can produce antibodies against antigens in cancer cells) or granzyme B secreting B-cells which could lead to tumor apoptosis could be also an interesting avenue for further research.

On the other hand, it should be determined how the immunosuppressive subsets of the B-cells infiltrate the RCC tissue. Immunosuppressive subsets of the B-cells like IL10- IL35- and TGF-β secreting Bregs the $CD19^{+}$B-cells or PD-L1 positive B-cells have not been well studied yet (Shen et al., 2016).

4.3 CD56 positive cells in ccRCC

Little is known about the role of the CD56+ cells in the immune response against RCC tumor cells. The present study showed that RCCs with higher peritumoral infiltration of the CD56 positive cells have a lower probability of developing a lymphovascular invasion.

CD56 cells were the only immune cell type in our study that showed an association with the lymphovascular tumor invasion. The association was only noticed for the peritumoral CD56-positive cells. Since the intratumoral CD56+ cells showed defect properties in different cancer subtypes, further studies should study the mechanisms leading to this deficient function.

Our data also showed a strong correlation between the CD56+ and the CD8+ positive cells. It is known that a proportion of the NK cells express CD8. This subtype of the NK cells has been shown to have increased efficiency in killing tumor cells (Wagner et al., 2019).

Further studies on the NK cells in RCC should also focus on the functional status of these cells, like the amount of secreted IFN-γ and TNF-α and the expression of CD16.

4.4 CD68 expression in ccRCC

CD68 is considered as general marker for the macrophages. We counted the macrophages in ccRCC and paired distant metastases and correlated the amount of intra and peritumoral macrophages with clinicopathological parameters.

However, the present study did not reveal associations between the CD68 density and the different clinicopathological parameters. By contrast, the study by (Nakanishi et al., 2018) showed a positive correlation between the CD68-positive cell density and each of the tumor stage, the Fuhrmann grade and the presence of metastases. In the same study, CD68+ cell density in ccRCC has been showed to be associated with worse prognosis**.** Previous data could also reveal that a higher TAMs density was associated with higher probability for tumor recurrence (Toge et al., 2009).

Macrophages can be divided into M1 and M2 macrophages. The different subtypes of the CD68+ macrophages has different effects regarding inducing or inhibiting the tumor growth (Komohara et al., 2011).

We did not differentiate in this study between M1 and M2 macrophages. Since CD68 is a general marker for macrophages, this could explain why the CD68+ cells in the present study did not show a correlation with the TNM clinicopathological parameters.

Our data showed that infiltration of the CD68 cells of the renal cancer tissue was higher compared to the metastatic sites. This could be attributed to the high production of the chemokine (C-X3-C motif) Ligand 1 (CX3CL1, also known as fractalkine) through several cells in the kidney like the glomerular endothelial cells the tubular epithelium and in less quantity other cells, such as podocytes, mesangial cells, renal tumor cells and stromal cells (Gottschalk and Kurts, 2015; Zhuang et al., 2017). This would increase the density of the monocytic cells in the kidney tissue. The renal mononuclear phagocytes express the chemokine receptor CX3CR1, which enhance its chemotaxis of toward the ligand CX3CL1. CX3CR1 is mostly expressed in the mononuclear phagocytes, while it is also expressed in some CD4+ and CD8+ T-cells, NK cells, NKT cells, and γδT cells. Moreover, the expression in human ccRCC cells was also reported (Vietinghoff and Kurts, 2021).

4.5 CD103+ cell infiltration in ccRCC

There are few investigations about CD103+ lymphocytes in ccRCC and no studies about the CD103+ lymphocytes infiltration in distant metastases. In comparing the composition of immune infiltrates in primary tumor and distant metastases, we found a significant accumulation of CD103+ lymphocytes in lung metastases, but not in metastases from other sites. This suggests that tissue memory resident cells accumulate in the lung tissue and could permit a rapid immunological answer (Abd Hamid et al., 2020) as well as an improved response to ICIs.

CD103+ cell infiltration has been shown to correlate with better outcomes in several tumors (Broz et al., 2014; Djenidi et al., 2015; Wang et al., 2015; Xiao et al., 2019). This study did not show statistical differences for the CD103 immune cell infiltration according to the T-stage, but our study revealed a higher CD103 peritumoral infiltration in the well-differentiated tumors. Nevertheless in the study by Wang et al. (2015) it has been demonstrated that the CD103 was inversely associated with the tumor size in bladder cancer.

The present study shows a strong correlation between the CD103 cells and each of CD8 and CD20 cells in the metastases (Pearson correlation of 0.7 for each) and an accumulation of CD103 cells in lung metastases. This prompts us to conclude that the infiltration of CD103 cells could have a positive impact on the immune recognition of the tumor antigens. Further studies should investigate the role of the tissue memory resident cells in ccRCC and metastases.

4.6 Tumor-infiltrating lymphocytes as prediction tool for metastatis

We assumed that a relatively high intratumoral immune cell infiltration compared to its peritumoral infiltration would be an indicator of better recognition of the tumor antigens through the immune system. We call this ratio the tumor infiltration ability index (TIAI).

TIAI of CD3 positiv-lymphocytes showed a significantly higher index in the primary tumors with distant metastases compared to the primary tumors without distant metastases. This fact negates our hypothesis, but could be explained by high immunogenity of ccRCC associated with the inhibition of T-lymphocytes, which was often described in ccRCC (Kim et al., 2021). This tumor ability index could be diagnostically useful to predict the occurrence of metastases, not only for RCC but this index could also a predictive diagnostic tool for the existence of metastasis in other types of solid tumors. These preliminary results should be investigated in larger samples of RCC as well in other solid tumor types.

After having compared tumor infiltration ability according to the grade of differentiation, we found that it was higher for CD8+ Cells in the well-differentiated tumors. This index could therefore also be useful as prognostic index, since tumors with higher TIAI could be a sign that these tumors are still under the control of the immune system.

4.7 Neuroendocrine differentiation of the ccRCC and its impact on the immune cell infiltration

Neuroendocrine differentiation could be found in a several cancers. CD56 belongs to the markers of neuroendocrine tumors. CD56 is a glycoprotein, that expressed early in development by many cell types. This glycoprotein influences a lot of cellular processes including proliferation differentiation and migration (Yap et al., 2017) . The overexpression of

CD56 on the tumor surface has been shown to correlate with tumor aggression (Gattenlöhner et al., 2009).

Small cell lung cancer, colon carcinoma, ovarian cancer, uterine carcinoma, malignant glioma, recurrent neuroblastoma, cutaneous malignant melanoma, gallbladder carcinoma, renal cell carcinoma and extrahepatic cholangiocarcinoma are all cancers that can express CD56 (Crossland et al., 2018; Weledji and Assob, 2014).

In our study about 26% of the tumors were positive for CD56, but no associations with tumor grade nor with the tumor size could be observed. Regarding the distant metastases, a CD56 tumor positivity was noticed often in cases with distant metastases (9/28 cases) compared with cases without distant metastases (4/22 cases). This CD56 positivity rate corresponds with the study results from (Ronkainen et al., 2010), which showed that 18 % of the RCC were positive for CD56. The same study did not reveal differences regarding the CD56 positivity with tumor stage nor with the tumor grade.

One of our striking results was that the CD56 positive tumors revealed a significant less frequent lymphocyte infiltration (for CD3+, CD4+, CD8+ and CD20+ cells). This difference in the infiltration was only present for the intratumoral immune cell infiltration, while peritumoral immune cell infiltration did not show significant differences. NCAM plays an important role in cell adhesion and formation of cell collectives in early embryonic cells (Weledji and Assob, 2014). An explanation for this impaired lymphocyte infiltration in CD56 positive tumors could be that the expression of CD56 in RCC induces the cell adhesion within the tumor tissue and therefore impairs the infiltration of the lymphocytes through the tumor.

As the CD56-negative cells were significantly more likely to have a rich immune cell infiltration, it is probably the case that these tumors would reveal a higher response to immunotherapies. Further studies on the effectiveness of the immunotherapies should consider the neuroendocrine differentiation and the tumor CD56 positivity.

It would also be interesting to know if the expression of other neuroendocrine markers on the RCC tumor cells like chromogranin and synaptophysin could also associate with altered the arrangement of the immune cells in the tumor microenvironment.

5. Summary

Primary ccRCCs and their distant metastases have a rich infiltrate of different subtypes of the immune cells, which have various effects on the immune response to the cancer and its outcome.

In this study, we performed a comprehensive analysis of immune cell infiltration in ccRCC, which revealed that the amount of intratumoral and peritumoral lymphocytes varies with each case.

We could show that the intratumoral and peritumoral immune cell infiltration is not affected by tumor stage in ccRCC, but the tumor grading was inversely associated with the amount of different subtypes of T-lymphocytes (CD4+ and CD8+). Regarding the infiltration with CD3+ cells, the peritumoral infiltration was significantly higher in the primary tumors of the M1 cases compared to M0 cases, but intratumoral tumor infiltration did not follow the same trend. We also found that B-cell infiltration inversely correlate with the occurrence of local lymph node metastasis. The absence of lymphovascular invasion was associated with higher peritumoral CD56 infiltration.

The tissue resident memory CD103+ lymphocytes accumulate in lung metastases and the CD68+ macrophages accumulate in bone metastases in comparison with other metastatic sites.

Surprisingly, CD56-positive RCCs showed less infiltration of B and T-lymphocytes. Our preliminary data also established an index for the tumor infiltration ability of the immune cells, which could predict a M0 status.

Understanding the immune system mechanisms against the RCC cells has led to new era of antitumor therapy. Further studies in this field are predicted to approve new medication groups and further improve the outcome in RCC patients.

6. List of figures

7. List of tables

8. References

Abd Hamid M, Colin-York H, Khalid-Alham N, Browne M, Cerundolo L, Chen J-L, Yao X, Rosendo-Machado S, Waugh C, Maldonado-Perez D, Bowes E, Verrill C, Cerundolo V, Conlon CP, Fritzsche M, Peng Y, Dong T. Self-Maintaining CD103+ Cancer-Specific T Cells Are Highly Energetic with Rapid Cytotoxic and Effector Responses. Cancer Immunol Res 2020; 8: 203–216

Arnett KL, Harrison SC, Wiley DC. Crystal structure of a human CD3-epsilon/delta dimer in complex with a UCHT1 single-chain antibody fragment. PNAS 2004; 101: 16268–16273

Baine MK, Turcu G, Zito CR, Adeniran AJ, Camp RL, Chen L, Kluger HM, Jilaveanu LB. Characterization of tumor infiltrating lymphocytes in paired primary and metastatic renal cell carcinoma specimens. Oncotarget 2015; 6: 24990–25002

Bersanelli M, Gnetti L, Varotti E, Ampollini L, Carbognani P, Leonardi F, Rusca M, Campanini N, Ziglioli F, Dadomo CI, Pilato FP, Cortellini A, Rapacchi E, Caruso G, Silini EM, Maestroni U, Buti S. Immune context characterization and heterogeneity in primary tumors and pulmonary metastases from renal cell carcinoma. Immunotherapy 2019; 11: 21–35

Broz ML, Binnewies M, Boldajipour B, Nelson AE, Pollack JL, Erle DJ, Barczak A, Rosenblum MD, Daud A, Barber DL, Amigorena S, Van't Veer LJ, Sperling AI, Wolf DM, Krummel MF. Dissecting the tumor myeloid compartment reveals rare activating antigen-presenting cells critical for T cell immunity. Cancer Cell 2014; 26: 638–652

Buti S, Bersanelli M, Sikokis A, Maines F, Facchinetti F, Bria E, Ardizzoni A, Tortora G, Massari F. Chemotherapy in metastatic renal cell carcinoma today? A systematic review. Anticancer Drugs 2013; 24: 535–554

Chevrier S, Levine JH, Zanotelli VRT, Silina K, Schulz D, Bacac M, Ries CH, Ailles L, Jewett MAS, Moch H, van den Broek M, Beisel C, Stadler MB, Gedye C, Reis B, Pe'er D, Bodenmiller B. An Immune Atlas of Clear Cell Renal Cell Carcinoma. Cell 2017; 169: 736-749.e18

Chistiakov DA, Killingsworth MC, Myasoedova VA, Orekhov AN, Bobryshev YV. CD68/macrosialin: not just a histochemical marker. Lab Invest 2017; 97: 4–13

Choi SYC, Collins CC, Gout PW, Wang Y. Cancer-generated lactic acid: a regulatory, immunosuppressive metabolite? J Pathol 2013; 230: 350–355

Choueiri TK, Powles T, Burotto M, Escudier B, Bourlon MT, Zurawski B, Oyervides Juárez VM, Hsieh JJ, Basso U, Shah AY, Suárez C, Hamzaj A, Goh JC, Barrios C, Richardet M, Porta C, Kowalyszyn R, Feregrino JP, Żołnierek J, Pook D, Kessler ER, Tomita Y, Mizuno R, Bedke J, Zhang J, Maurer MA, Simsek B, Ejzykowicz F, Schwab GM, Apolo AB, Motzer RJ. Nivolumab plus Cabozantinib versus Sunitinib for Advanced Renal-Cell Carcinoma. N Engl J Med 2021; 384: 829–841

Cózar B, Greppi M, Carpentier S, Narni-Mancinelli E, Chiossone L, Vivier E. Tumor-Infiltrating Natural Killer Cells. Cancer Discov 2020

Cragg MS, Walshe CA, Ivanov AO, Glennie MJ. The biology of CD20 and its potential as a target for mAb therapy. Curr Dir Autoimmun 2005; 8: 140–174

Crossland DL, Denning WL, Ang S, Olivares S, Mi T, Switzer K, Singh H, Huls H, Gold KS, Glisson BS, Cooper LJ, Heymach JV. Antitumor activity of CD56-chimeric antigen receptor T cells in neuroblastoma and SCLC models. Oncogene 2018; 37: 3686–3697

Dabestani S, Thorstenson A, Lindblad P, Harmenberg U, Ljungberg B, Lundstam S. Renal cell carcinoma recurrences and metastases in primary non-metastatic patients: a population-based study. World J Urol 2016; 34: 1081–1086

Daurkin I, Eruslanov E, Stoffs T, Perrin GQ, Algood C, Gilbert SM, Rosser CJ, Su L-M, Vieweg J, Kusmartsev S. Tumor-associated macrophages mediate immunosuppression in the renal cancer microenvironment by activating the 15-lipoxygenase-2 pathway. Cancer Res 2011; 71: 6400–6409

Delahunt B, Cheville JC, Martignoni G, Humphrey PA, Magi-Galluzzi C, McKenney J, Egevad L, Algaba F, Moch H, Grignon DJ, Montironi R, Srigley JR. The International Society of

Urological Pathology (ISUP) grading system for renal cell carcinoma and other prognostic parameters. Am J Surg Pathol 2013; 37: 1490–1504

Djenidi F, Adam J, Goubar A, Durgeau A, Meurice G, Montpréville V de, Validire P, Besse B, Mami-Chouaib F. CD8+CD103+ tumor-infiltrating lymphocytes are tumor-specific tissue-resident memory T cells and a prognostic factor for survival in lung cancer patients. J Immunol 2015; 194: 3475–3486

Dutcher JP. Update on the biology and management of renal cell carcinoma. J Investig Med 2019; 67: 1–10

EAU Guidelines. Edn. presented at the EAU Annual Congress Amsterdam 2022. ISBN 978-94-92671-16-5)

Fregni G, Perier A, Avril M-F, Caignard A. NK cells sense tumors, course of disease and treatments: Consequences for NK-based therapies. Oncoimmunology 2012; 1: 38–47

Fuhrman SA, Lasky LC, Limas C. Prognostic significance of morphologic parameters in renal cell carcinoma. Am J Surg Pathol 1982; 6: 655–663

Gattenlöhner S, Stühmer T, Leich E, Reinhard M, Etschmann B, Völker H-U, Rosenwald A, Serfling E, Bargou RC, Ertl G, Einsele H, Müller-Hermelink H-K. Specific detection of CD56 (NCAM) isoforms for the identification of aggressive malignant neoplasms with progressive development. Am J Surg Pathol 2009; 174: 1160–1171

Ghadially H, Ross X-L, Kerst C, Dong J, Reske-Kunz AB, Ross R. Differential regulation of CCL22 gene expression in murine dendritic cells and B cells. J Immunol 2005; 174: 5620–5629

Giraldo NA, Becht E, Pagès F, Skliris G, Verkarre V, Vano Y, Mejean A, Saint-Aubert N, Lacroix L, Natario I, Lupo A, Alifano M, Damotte D, Cazes A, Triebel F, Freeman GJ, Dieu-Nosjean M-C, Oudard S, Fridman WH, Sautès-Fridman C. Orchestration and Prognostic Significance of Immune Checkpoints in the Microenvironment of Primary and Metastatic Renal Cell Cancer. Clin Cancer Res 2015; 21: 3031–3040

Gottfried E, Kunz-Schughart LA, Weber A, Rehli M, Peuker A, Müller A, Kastenberger M, Brockhoff G, Andreesen R, Kreutz M. Expression of CD68 in non-myeloid cell types. Scand J Immunol 2008; 67: 453–463

Gottschalk C, Kurts C. The Debate about Dendritic Cells and Macrophages in the Kidney. Front Immunol 2015; 6: 435

Gray RE, Harris GT. Renal Cell Carcinoma: Diagnosis and Management. Am Fam Physician 2019; 99: 179–184

Guo C, Zhao H, Wang Y, Bai S, Yang Z, Wei F, Ren X. Prognostic Value of the Neo-Immunoscore in Renal Cell Carcinoma. Front Oncol 2019; 9: 439

Henriksen KJ, Chang A. The Importance of Nephropathology in Kidney Cancer. Semin Nephrol 2020; 40: 69–75

Huber V, Camisaschi C, Berzi A, Ferro S, Lugini L, Triulzi T, Tuccitto A, Tagliabue E, Castelli C, Rivoltini L. Cancer acidity: An ultimate frontier of tumor immune escape and a novel target of immunomodulation. Semin Cancer Biol 2017; 43: 74–89

Kim M-C, Jin Z, Kolb R, Borcherding N, Chatzkel JA, Falzarano SM, Zhang W. Updates on Immunotherapy and Immune Landscape in Renal Clear Cell Carcinoma. Cancers (Basel) 2021; 13

Kobayashi T, Hamaguchi Y, Hasegawa M, Fujimoto M, Takehara K, Matsushita T. B cells promote tumor immunity against B16F10 melanoma. Am J Pathol 2014; 184: 3120–3129

King SC, Pollack LA, Li J, King JB, Master VA. Continued increase in incidence of renal cell carcinoma, especially in young patients and high grade disease: United States 2001 to 2010. J Urol 2014; 191: 1665–1670

Komohara Y, Hasita H, Ohnishi K, Fujiwara Y, Suzu S, Eto M, Takeya M. Macrophage infiltration and its prognostic relevance in clear cell renal cell carcinoma. Cancer Sci 2011; 102: 1424–1431

Kovaleva OV, Samoilova DV, Shitova MS, Gratchev A. Tumor Associated Macrophages in Kidney Cancer. Anal Cell Pathol (Amst) 2016; 2016

Ladányi A. Prognostic and predictive significance of immune cells infiltrating cutaneous melanoma. Pigment Cell Melanoma Res 2015; 28: 490–500

Milne K, Köbel M, Kalloger SE, Barnes RO, Gao D, Gilks CB, Watson PH, Nelson BH. Systematic analysis of immune infiltrates in high-grade serous ovarian cancer reveals CD20, FoxP3 and TIA-1 as positive prognostic factors. PLoS One 2009; 4: e6412

Motzer RJ, Mazumdar M, Bacik J, Berg W, Amsterdam A, Ferrara J. Survival and prognostic stratification of 670 patients with advanced renal cell carcinoma. J Clin Oncol 1999; 17: 2530–2540

Nagorsen D, Voigt S, Berg E, Stein H, Thiel E, Loddenkemper C. Tumor-infiltrating macrophages and dendritic cells in human colorectal cancer: relation to local regulatory T cells, systemic T-cell response against tumor-associated antigens and survival. J Transl Med 2007; 5: 62

Nakanishi H, Miyata Y, Mochizuki Y, Yasuda T, Nakamura Y, Araki K, Sagara Y, Matsuo T, Ohba K, Sakai H. Pathological significance and prognostic roles of densities of CD57+ cells, CD68+ cells, and mast cells, and their ratios in clear cell renal cell carcinoma. Hum Pathol 2018; 79: 102–108

Nutt SL, Hodgkin PD, Tarlinton DM, Corcoran LM. The generation of antibody-secreting plasma cells. Nat Rev Immunol 2015; 15: 160–171

Padala SA, Barsouk A, Thandra KC, Saginala K, Mohammed A, Vakiti A, Rawla P, Barsouk A. Epidemiology of Renal Cell Carcinoma. World J Oncol 2020; 11: 79–87

Parikh M, Bajwa P. Immune Checkpoint Inhibitors in the Treatment of Renal Cell Carcinoma. Semin Nephrol 2020; 40: 76–85

Petricevic B, Laengle J, Singer J, Sachet M, Fazekas J, Steger G, Bartsch R, Jensen-Jarolim E, Bergmann M. Trastuzumab mediates antibody-dependent cell-mediated cytotoxicity and

phagocytosis to the same extent in both adjuvant and metastatic HER2/neu breast cancer patients. J Transl Med 2013; 11: 307

Raskov H, Orhan A, Christensen JP, Gögenur I. Cytotoxic CD8+ T cells in cancer and cancer immunotherapy. Br J Cancer 2021; 124: 359–367

Rasmussen F. Metastatic renal cell cancer. Cancer Imaging 2013; 13: 374–380

Rassy E, Flippot R, Albiges L. Tyrosine kinase inhibitors and immunotherapy combinations in renal cell carcinoma. Ther Adv Med Oncol 2020; 12: 1758835920907504

Rini BI, Powles T, Atkins MB, Escudier B, McDermott DF, Suarez C, Bracarda S, Stadler WM, Donskov F, Lee JL, Hawkins R, Ravaud A, Alekseev B, Staehler M, Uemura M, Giorgi U de, Mellado B, Porta C, Melichar B, Gurney H, Bedke J, Choueiri TK, Parnis F, Khaznadar T, Thobhani A, Li S, Piault-Louis E, Frantz G, Huseni M, Schiff C, Green MC, Motzer RJ. Atezolizumab plus bevacizumab versus sunitinib in patients with previously untreated metastatic renal cell carcinoma (IMmotion151): a multicentre, open-label, phase 3, randomised controlled trial. Lancet 2019; 393: 2404–2415

Ronkainen H, Soini Y, Vaarala MH, Kauppila S, Hirvikoski P. Evaluation of neuroendocrine markers in renal cell carcinoma. Diagn Pathol 2010; 5: 28

Sanders C, Hamad ASM, Ng S, Hosni R, Ellinger J, Klümper N, Ritter M, Stephan C, Jung K, Hölzel M, Kristiansen G, Hauser S, Toma MI. CD103+ Tissue Resident T-Lymphocytes Accumulate in Lung Metastases and Are Correlated with Poor Prognosis in ccRCC. Cancers (Basel) 2022; 14

Sasidharan Nair V, Elkord E. Immune checkpoint inhibitors in cancer therapy: a focus on T-regulatory cells. Immunol Cell Biol 2018; 96: 21–33

Selvi I, Demirci U, Bozdogan N, Basar H. The prognostic effect of immunoscore in patients with clear cell renal cell carcinoma: preliminary results. Int Urol Nephrol 2020; 52: 21–34

Senovilla L, Vacchelli E, Galon J, Adjemian S, Eggermont A, Fridman WH, Sautès-Fridman C, Ma Y, Tartour E, Zitvogel L, Kroemer G, Galluzzi L. Trial watch: Prognostic and predictive value of the immune infiltrate in cancer. Oncoimmunology 2012; 1: 1323–1343

Sharonov GV, Serebrovskaya EO, Yuzhakova DV, Britanova OV, Chudakov DM. B cells, plasma cells and antibody repertoires in the tumour microenvironment. Nat Rev Immunol 2020; 20: 294–307

Shen M, Sun Q, Wang J, Pan W, Ren X. Positive and negative functions of B lymphocytes in tumors. Oncotarget 2016; 7: 55828–55839

Siegel RL, Miller KD, Jemal A. Cancer statistics, 2018. CA Cancer J Clin 2018; 68: 7–30

Singer K, Kastenberger M, Gottfried E, Hammerschmied CG, Büttner M, Aigner M, Seliger B, Walter B, Schlösser H, Hartmann A, Andreesen R, Mackensen A, Kreutz M. Warburg phenotype in renal cell carcinoma: high expression of glucose-transporter 1 (GLUT-1) correlates with low CD8(+) T-cell infiltration in the tumor. Int J Cancer 2011; 128: 2085–2095

Sjöberg E, Frödin M, Lövrot J, Mezheyeuski A, Johansson M, Harmenberg U, Egevad L, Sandström P, Östman A. A minority-group of renal cell cancer patients with high infiltration of CD20+B-cells is associated with poor prognosis. Br J Cancer 2018; 119: 840–846

Stenzel PJ, Schindeldecker M, Tagscherer KE, Foersch S, Herpel E, Hohenfellner M, Hatiboglu G, Alt J, Thomas C, Haferkamp A, Roth W, Macher-Goeppinger S. Prognostic and Predictive Value of Tumor-infiltrating Leukocytes and of Immune Checkpoint Molecules PD1 and PDL1 in Clear Cell Renal Cell Carcinoma. Transl Oncol 2019; 13: 336–345

Toge H, Inagaki T, Kojimoto Y, Shinka T, Hara I. Angiogenesis in renal cell carcinoma: the role of tumor-associated macrophages. Int J Urol I 2009; 16: 801–807

Vietinghoff S von, Kurts C. Regulation and function of CX3CR1 and its ligand CX3CL1 in kidney disease. Cell Tissue Res 2021

Wagner AK, ALICI E, LOWDELL MW. Characterization of human natural killer cells for therapeutic use. Cytotherapy 2019; 21: 315–326

Wang B, Wu S, Zeng H, Liu Z, Dong W, He W, Chen X, Dong X, Zheng L, Lin T, Huang J. CD103+ Tumor Infiltrating Lymphocytes Predict a Favorable Prognosis in Urothelial Cell Carcinoma of the Bladder. J Urol 2015; 194: 556–562

Warren AY, Harrison D. WHO/ISUP classification, grading and pathological staging of renal cell carcinoma: standards and controversies. World J Urol 2018; 36: 1913–1926

Wei X, Jin Y, Tian Y, Zhang H, Wu J, Lu W, Lu X. Regulatory B cells contribute to the impaired antitumor immunity in ovarian cancer patients. Tumour Biol 2016; 37: 6581–6588

Weledji EP, Assob JC. The ubiquitous neural cell adhesion molecule (N-CAM). Ann Med Surg (Lond) 2014; 3: 77–81

Wettersten HI, Hakimi AA, Morin D, Bianchi C, Johnstone ME, Donohoe DR, Trott JF, Aboud OA, Stirdivant S, Neri B, Wolfert R, Stewart B, Perego R, Hsieh JJ, Weiss RH. Grade-Dependent Metabolic Reprogramming in Kidney Cancer Revealed by Combined Proteomics and Metabolomics Analysis. Cancer Res 2015; 75: 2541–2552

Wittekind C. TNM - Klassifikation maligner Tumoren, Reg. Weinheim: Wiley-VCH, 2020

Wolf MM, Kimryn Rathmell W, Beckermann KE. Modeling clear cell renal cell carcinoma and therapeutic implications. Oncogene 2020

Xiao Y, Li H, Mao L, Yang QC, Fu LQ, Wu CC, Liu B, Sun ZJ. CD103+ T and Dendritic Cells Indicate a Favorable Prognosis in Oral Cancer. J Dent Res 2019; 98: 1480–1487

Yap L-W, Brok J, Pritchard-Jones K. Role of CD56 in Normal Kidney Development and Wilms Tumorigenesis. Fetal Pediatr Pathol 2017; 36: 62–75

Zhang S, Zhang E, Long J, Hu Z, Peng J, Liu L, Tang F, Li L, Ouyang Y, Zeng Z. Immune infiltration in renal cell carcinoma. Cancer Sci 2019; 110: 1564–1572

Zhao Y, Ge X, Xu X, Yu S, Wang J, Sun L. Prognostic value and clinicopathological roles of phenotypes of tumour-associated macrophages in colorectal cancer. J Cancer Res Clin Oncol 2019; 145: 3005–3019

Zhou X, Su Y-X, Lao X-M, Liang Y-J, Liao G-Q. CD19(+)IL-10(+) regulatory B cells affect survival of tongue squamous cell carcinoma patients and induce resting CD4(+) T cells to CD4(+)Foxp3(+) regulatory T cells. Oral Oncol 2016; 53: 27–35

Zhuang Q, Cheng K, Ming Y. CX3CL1/CX3CR1 Axis, as the Therapeutic Potential in Renal Diseases: Friend or Foe? Curr Gene Ther 2017; 17: 442–452

9. Acknowledgements

I would like to thank my parents, who supported me to achieve success in every part of my life. I would like to thank my doctoral supervisor, Prof. Dr. med. Toma, who supported me all the time during the experimental part and during writing this dissertation.

In addition, I would like to thank Susanne Steiner and Carsten Golletz for their excellent technical assistance.

Last but not least, I would like to thank Prof. Dr. med. Kristiansen for his constant support and encouragement.